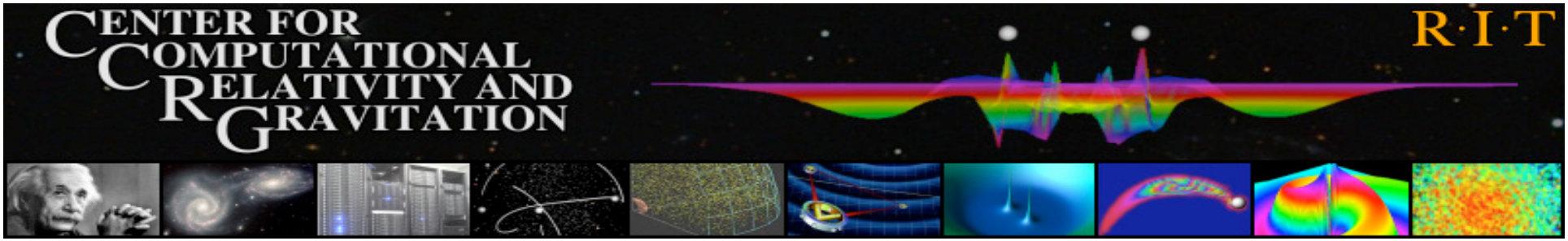

Full Numerical Simulation of Astrophysical Binary Black Hole Mergers

Carlos Lousto

Center for Computational Relativity and Gravitation

http://ccrg.rit.edu

Rochester Institute of Technology

Southampton, UK
July 8th, 2011

Overview

- Brief History of NR breakthroughs
- Main NR results for BBH dynamics
- Unequal mass cases
  - Full numerical simulations
  - NR + Perturbation theory

Simulation of Black-Hole Binaries with Full Numerical General Relativity

- Numerical Relativity:
  - Solve numerically the full GR eqs for dynamical spacetime, in strong gravity where no approximations hold.
  - Very difficult problem …
- Goals:
  - Understand gravity at its strongest manifestation
  - Inform gravitational wave detection
  - Determine characteristics of compact objects (final black hole)
- Challenges:
  - Several scales required for physics
    - Mass of the smallest BH, BH spins, etc
    - Wavelength of the waveform in the wave zone
  - Long waveforms matching early PN inspiral
  - Large parameter space: mass ratio, spins, eccentricity …

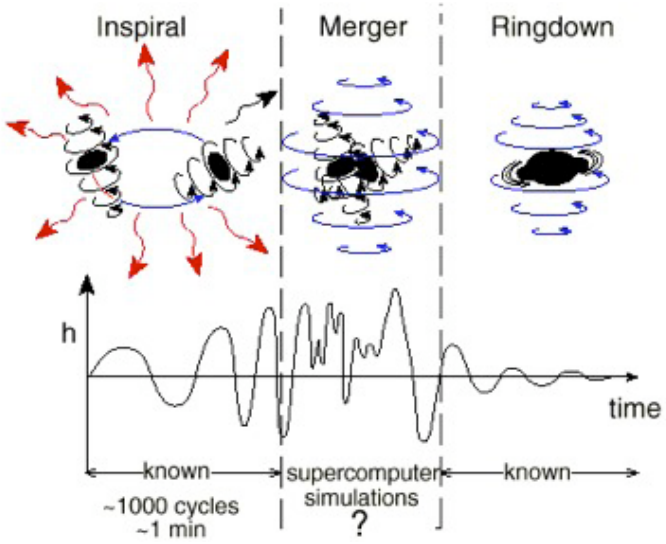

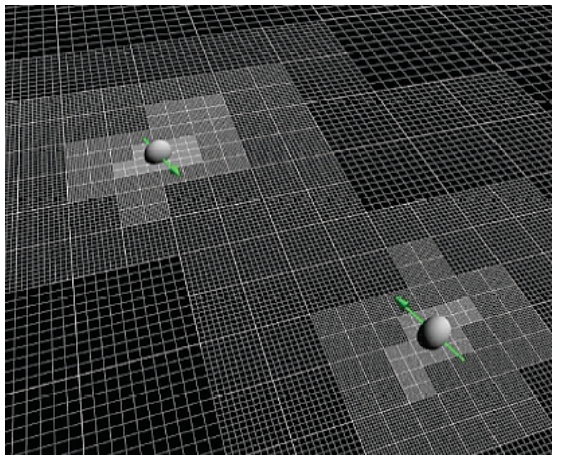

Credits: NASA GSFC group, 2007

Numerical Relativity: 30-40 years of challenges

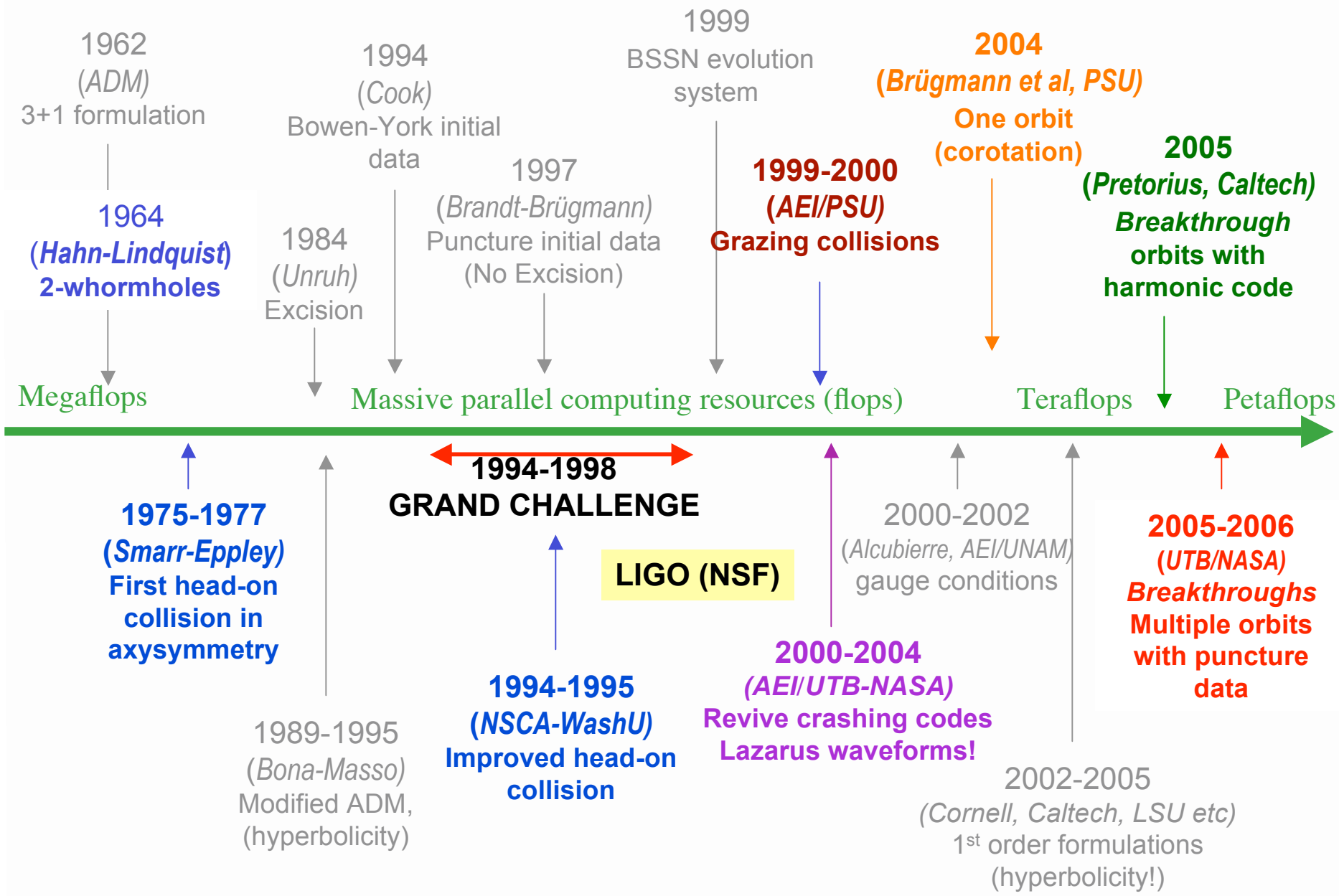

A Brief Historical Overview

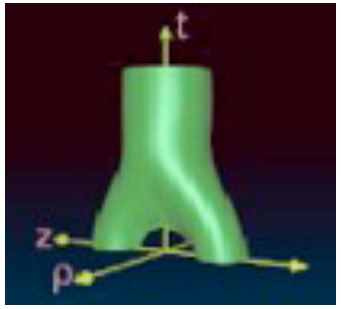

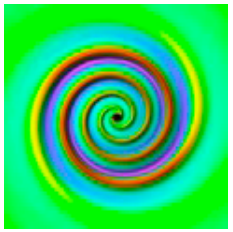

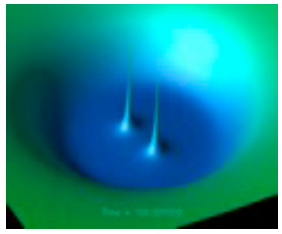

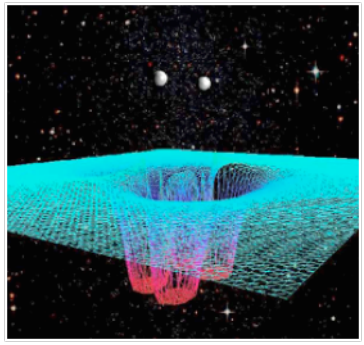

40+years of hard labor:

1964 First Simulation (Hahn & Lindquist)

… then LIGO …

1990s Grand Challenge

BSSN-NOK evolution system

Puncture Initial Data (Brandt-Bruegman)

Gauge: Fixed Punctures (Alcubierre et al.)

Lazarus (Campanelli et al)

2004 One Orbit (Buegman et al.)

Breakthrough:

2005 Binary Inspiral and Merger

Pretorius, PRL 95 (2005)

2006 Moving Punctures (RIT & NASA)

Campanelli et al PRL 96 (2006)

Baker et al PRL 96, (2006)

Numerical Relativity today:

2006+ GW Waveforms & Orbits,

Spin dynamics, Mass ratios,

GW Recoils, BH remnants,

BHs multiplets

2009+ Community Collaborations

2010+ Extreme BH Binaries

BH Binaries in a gaseous environment

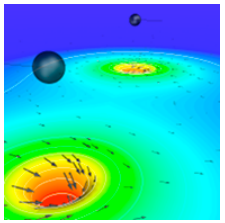

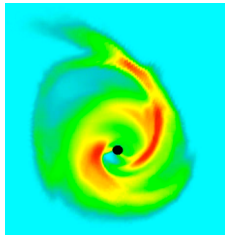

Spectral Einstein Code (SpEC):

Generalized Harmonic, but 1st order

Physical BCs

Highly-accurate, but less flexible (care needed to get BH-BH merger)

Extended to GRMHD (BH-NS, Duez)

Moving Puncture Codes:

BSSN + Punctures, AMR

Less-accurate, but more flexible and robust (NBBH -BH/NS mergers)

Community Codes, including GRMHD (http://einsteintoolkit.org)

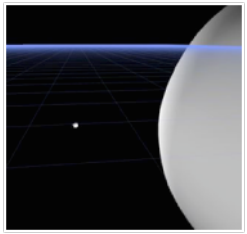

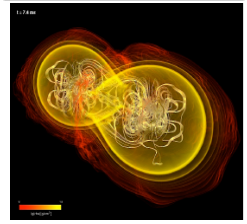

The conformal BSSN system with moving punctures

Modified BSSN system:

$$
\begin{aligned}
\partial_0 \tilde{\gamma}_{ij} &= -2\alpha \tilde{A}_{ij}, \qquad \partial_0 = \partial_t - \mathcal{L}_\beta, \\
\partial_t \chi &= \frac{2}{3}\chi\left(\alpha K - \partial_a \beta^a\right) + \beta^i \partial_i \chi, \\
\partial_0 \tilde{A}_{ij} &= \chi\left(-D_i D_j \alpha + \alpha R_{ij}\right)^{TF} + \\
&\quad \alpha\left(K\tilde{A}_{ij} - 2\tilde{A}_{ik}\tilde{A}^k_j\right), \\
\partial_0 K &= -D^i D_i \alpha + \alpha\left(\tilde{A}_{ij}\tilde{A}^{ij} + \frac{1}{3}K^2\right), \\
\partial_t \tilde{\Gamma}^i &= \tilde{\gamma}^{jk}\partial_j\partial_k\beta^i + \frac{1}{3}\tilde{\gamma}^{ij}\partial_j\partial_k\beta^k + \beta^j\partial_j\tilde{\Gamma}^i - \\
&\quad \tilde{\Gamma}^j\partial_j\beta^i + \frac{2}{3}\tilde{\Gamma}^i\partial_j\beta^j - 2\tilde{A}^{ij}\partial_j\alpha + \\
&\quad 2\alpha\left(\tilde{\Gamma}^i_{jk}\tilde{A}^{jk} + 6\tilde{A}^{ij}\partial_j\phi - \frac{2}{3}\tilde{\gamma}^{ij}\partial_j K\right), \\
\tilde{\Gamma}^i &= -\partial_j\tilde{\gamma}^{ij}.
\end{aligned}
$$

Replace ϕ $(O(\log r))$ with $\chi = e^{-4\phi}$ $(O(r^4))$

$\partial_0\alpha = -2\alpha K$

$\partial_t\beta^a = B^a$, $\partial_t B^a = 3/4\partial_t\tilde{\Gamma}^a - \eta B^a$

$\alpha(t=0) = \psi_{BL}^{-2} \qquad \beta^i = B^i = 0.$

Numerical Code: LazEv

- Modular
  - Cactus-based framework
- Flexible
  - *Mathematica* scripts used to generate C routines (257108 lines)
- Use 8th order finite differencing in space with MoL integration
  - standard 8th order centered stencils for all spatial derivatives
  - upwinded 4th order stencils for the advection (shift) terms
  - standard 4th order RK for time evolution

The Moving Puncture Approach

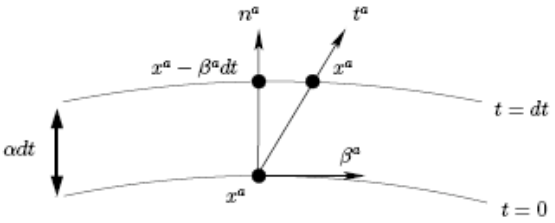

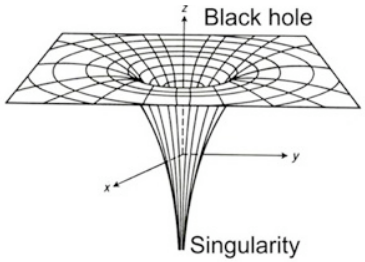

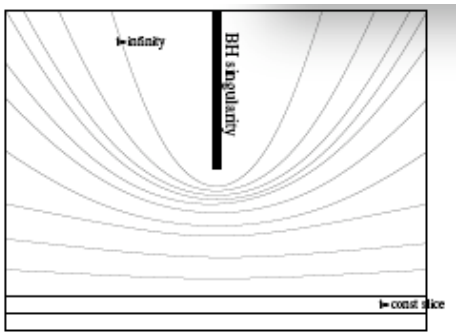

- The formalism: "3+1" approach [Arnowitt, Deser and Misner, 1962]
- BH "puncture" initial data (no-excision) [Brandt & Brügmann, 1997]
- Strongly hyperbolic BSSN evolution system [Nakamura-Oohara-Kojima (1987), Shibata-Nakamura (1995), Baumgarte-Shapiro (1999)]
  - 17 variables g_{ij}, $A_{ij} \sim \partial_t g_{ij}$, Φ, K, Γ^i
- New variables that regularize the puncture: $W = e^{-2\phi}$
- Modified Gauges to allow punctures to move across grid
  - Singularity avoiding
  - Coordinate not too distorted
  - Gridpoint should resolve region of interest

$$(\partial_t - \beta^i \partial_i)\alpha = -2\alpha K$$
$$\partial_t \beta^i = 3/4\tilde{\Gamma}^i - \eta\beta^i$$

- Numerics:
  - Method of Lines Integration: RK4 time integration, 8th-order spatial finite differencing, with Kreiss-Oliger dissipation.
  - Many Scales in the problem: parallelization (MPI) and AMR techniques (moving boxes).
- Extraction of physics quantities "at infinity" and at the BH horizons, such as conserved masses, momenta and spins, as well as radiation waveform, energy, angular and linear momenta.

$$\Psi_4 = \ddot{h}_+ - i\ddot{h}_\times$$

$$h = h_+ + ih_\times .$$

$$h \sim \frac{G}{c^4}\frac{\ddot{Q}}{r} \sim \frac{GM_{\rm quad}}{rc^2}\frac{v^2}{c^2},$$

Merger of Spinning Black Holes: Hang-Up Orbits

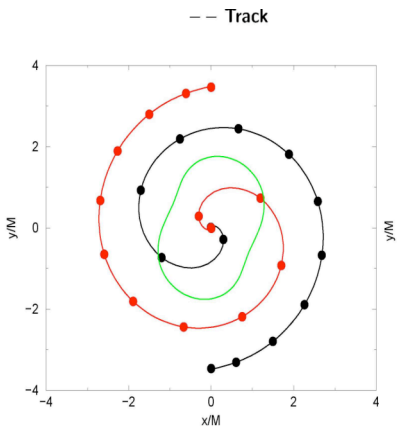

Figure 4: Puncture tracks for the – – configuration.

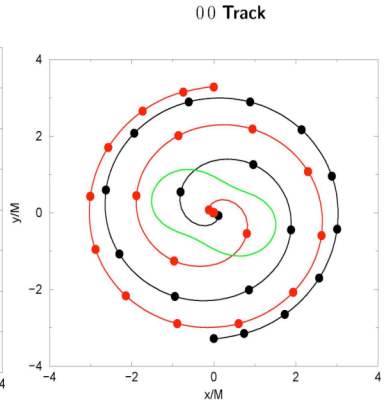

Figure 5: Puncture tracks for the 00 configuration.

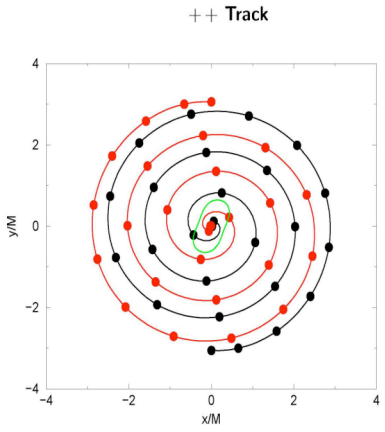

Figure 6: Puncture tracks for the ++ configuration.

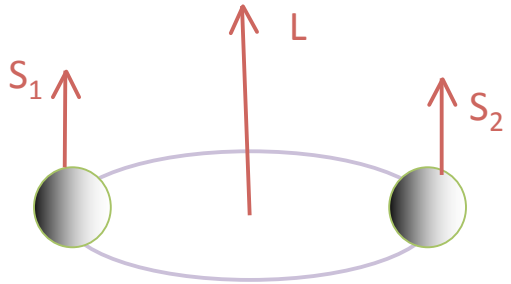

- Equal-mass BHBs
- $S_{1,2}/m^2 = \{-0.75, 0, 0.75\}$
- $M\Omega = 0.05$ (Starting "radius" the same).

- Hang-up effect due to repulsive spin-orbit interaction leaving behind a remnant with sub-maximal spin <0.96) [Campanelli, Lousto, Zlochower, PRD 2006]: cosmic censorship respected!

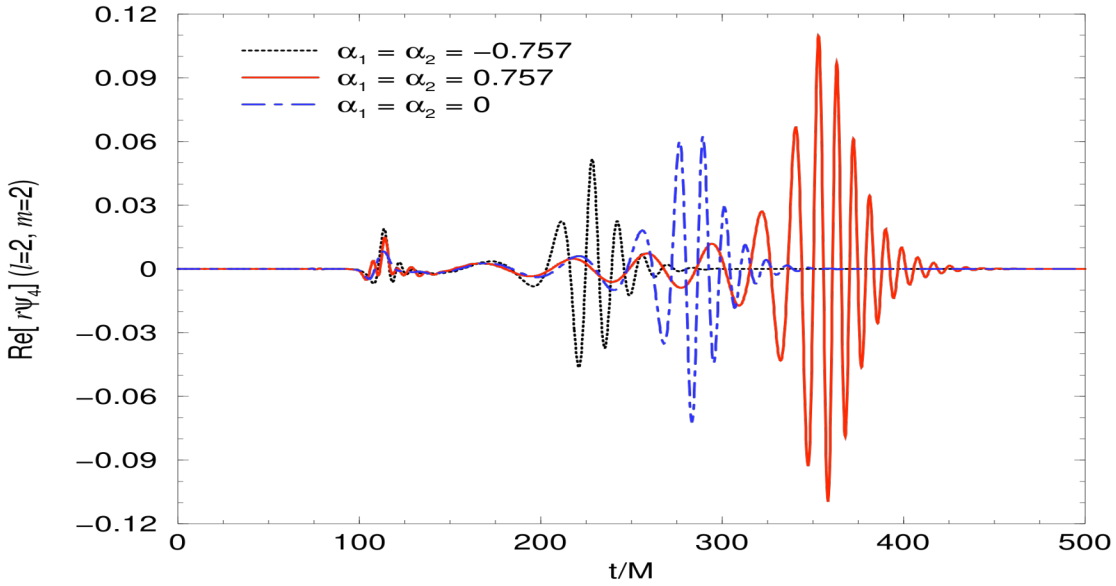

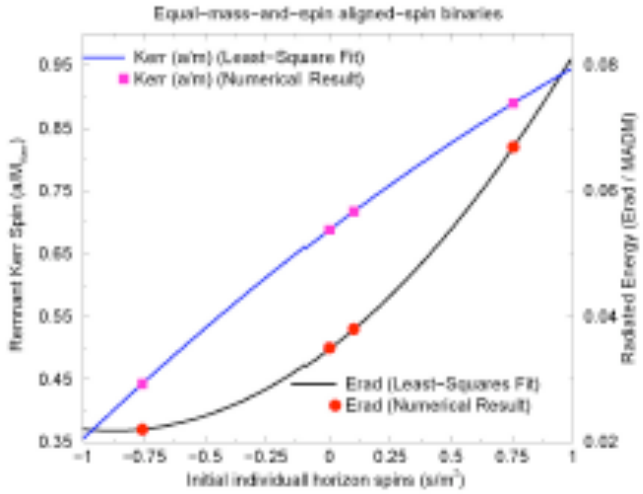

Exploring BH Merger Spin Dynamics

• Merger of a generic, precessing BH binary [Campanelli, Lousto, Nakano and Zlochower, PRD 2009]

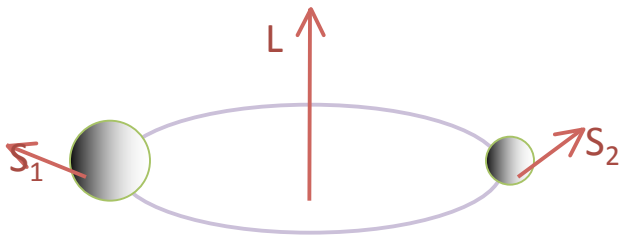

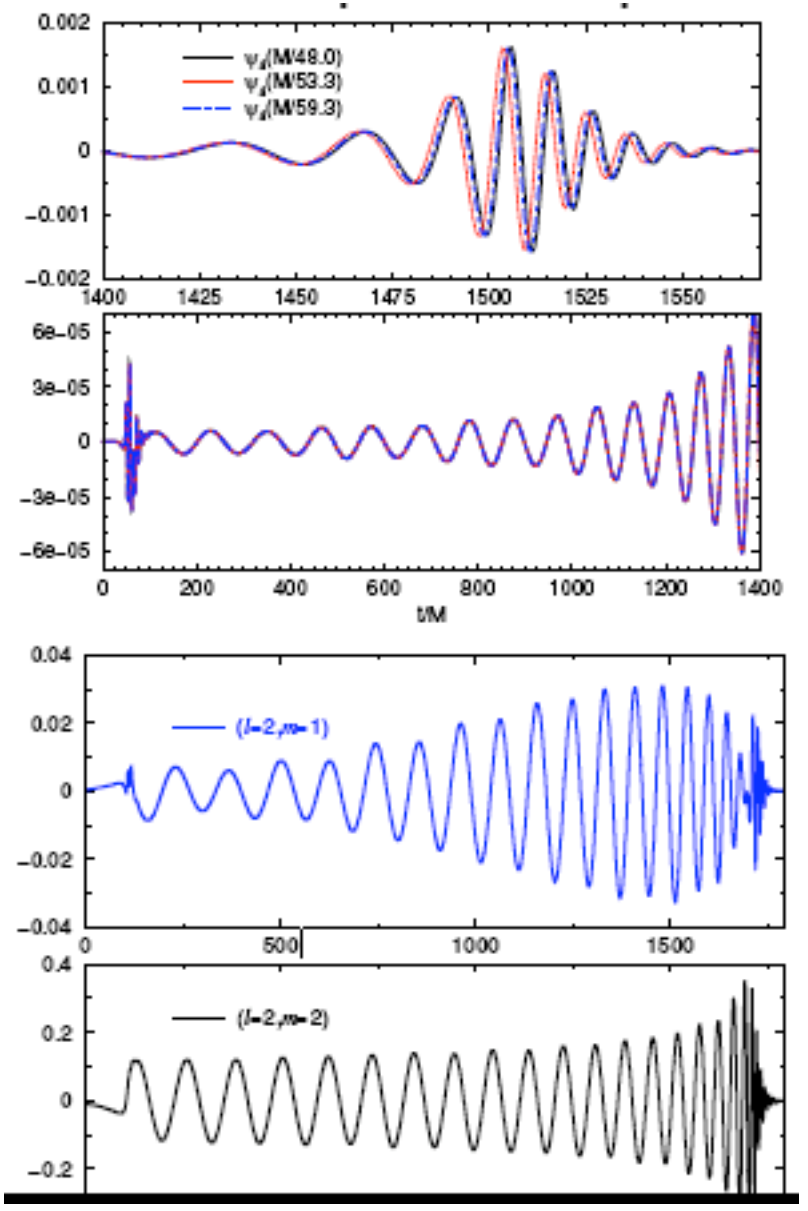

• Random Spin, non-equal mass, small eccentricity
- m_1/m_2 ~ 0.8, a_1/m_1 ~ 0.6, a_2/m_2 ~ 0.4
- spins initially at arbitrary orientations
- complete 9 orbits prior merger
- initial parameters from 3.5PN inspiral evolution (> 300 orbits)

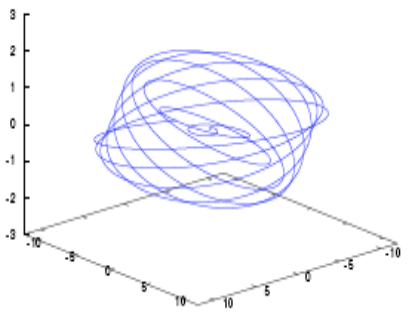

Trajectory difference $\underline{r} = \underline{x}_1 - \underline{x}_2$

• These Simulations are Computationally Challenging!

- Large simulations .. 1000s of CPUs, many TBs of data
- Need highly-efficient AMR (very different length scales)
- Need high accuracy to get small BH dynamics
- Spinning data requires much higher resolutions

Kick from a Generic Astrophysical BH binary

- In astrophysical, quasi-circular, spinning BH binaries mergers, such kicks can be as large as 3,680 km/s [Campanelli et al, ApJL 2007, Campanelli et al, PRL 2007, Lousto & Zlochower, PRD, 2010]

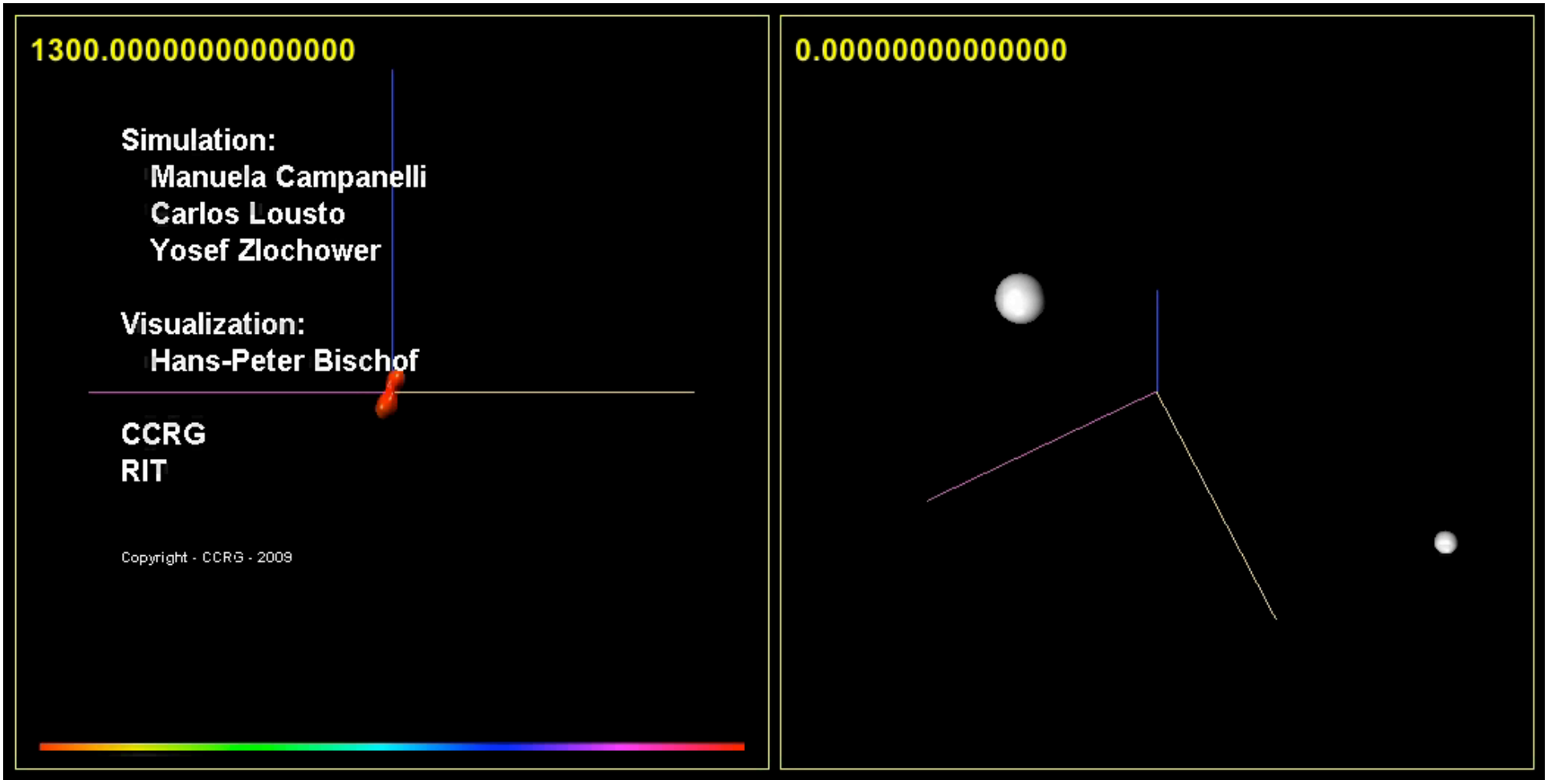

Radiated power (Left), Orbit and Kick (Right)

Large merger recoils from precessing quasi-circular binaries

Generic binary displaying significant precession of spin axis is observed to produce a large recoil kick at merger [Campanelli et al, APJ Lett 2007]

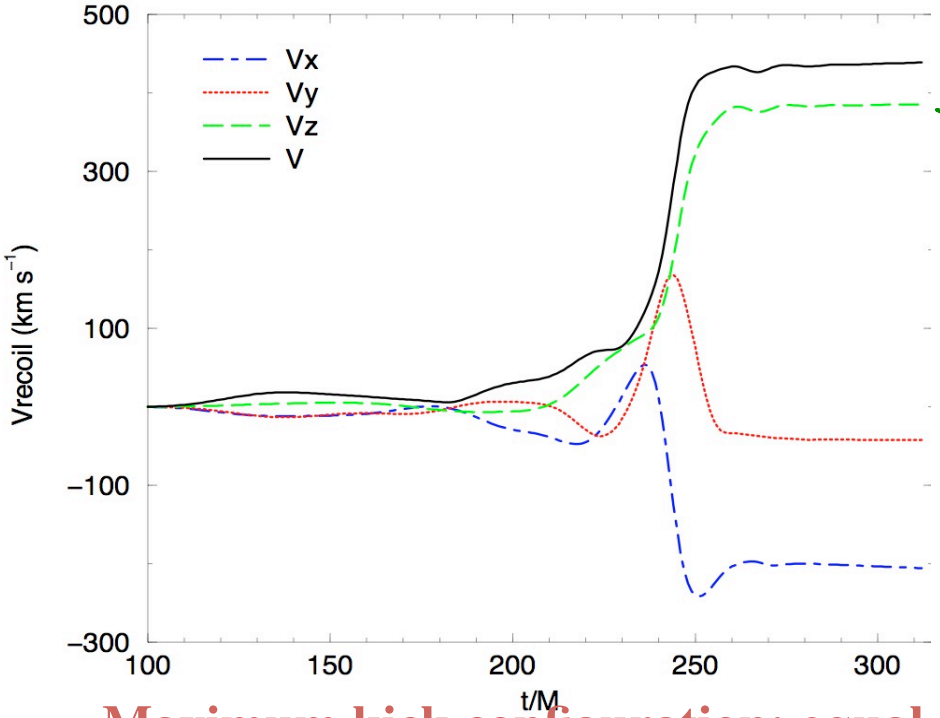

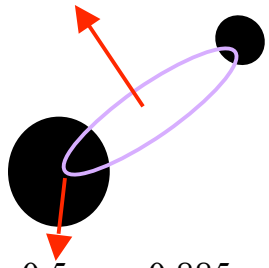

SP6: q = 0.5, a_1= 0.885, a_2 = 0

"... the spin component to the recoil velocity may produce the leading contribution. This is suggested by the fact that the z-component of the recoil, which is not present for non-spinning binaries, is the dominant component ..."

Maximum kick configuration: equal-mass circular binaries with opposite in-plane spins produce large out-of-plane kicks

- Following:

  [Gonzalez et al, Phys. Rev. Lett, 2007] calculate kick of 2500 km/s

  [Campanelli et al, Phys. Rev. Lett, 2007] predicts kicks up to 4000 km/s

  [Dain, et al, Phys. Rev. D 2008] calculate 3300 km/s for nearly maximal spins

The Superkick Configurations

- In quasi-circular BH binaries, the largest kicks are obtained when BH spins within the orbital plane, equal in magnitude, but opposite in direction

  - The resultant recoil velocity depends sinusoidally on the initial phase of the binary, and linearly (at leading order) on the magnitude of the individual BH spins [Campanelli et al, 2007]

  - The "bobbing" motion of the orbit causes an asymmetric beaming of the radiation produced by the in-plane orbital motion of the binary, and the net asymmetry is balanced by a recoil [Sperhake et al, 2010]

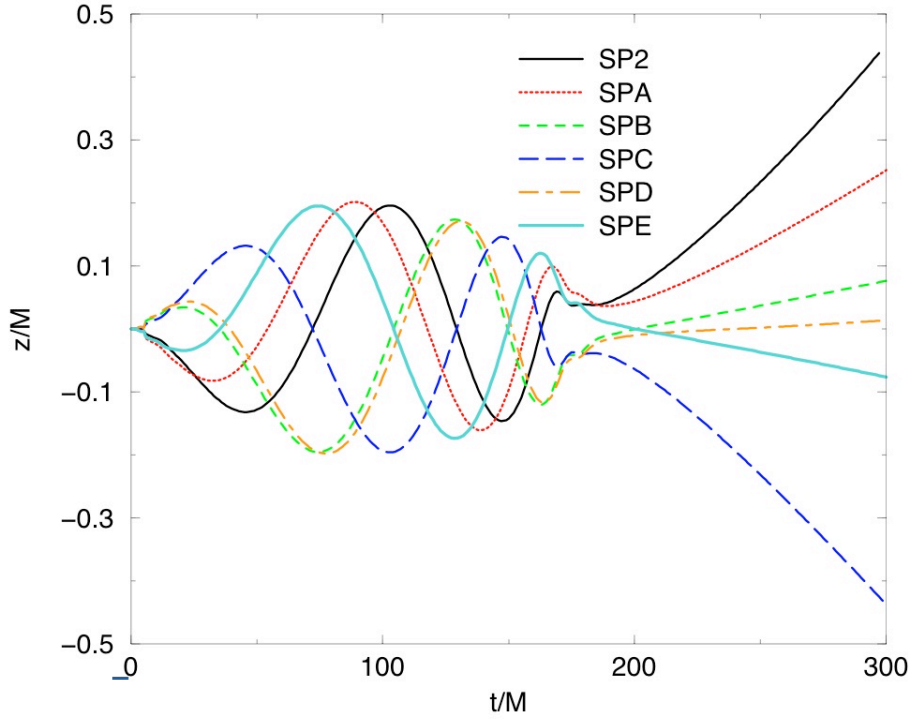

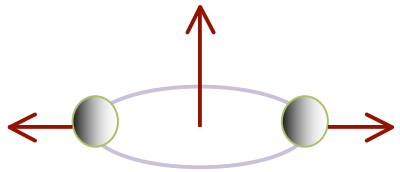

  - Schematic explanations: Effect due to frame dragging of one BH relative to the other and viceversa [Pretorius, 2008]; spin-curvature coupling [Keppel et al, 2009]; kinematical spin effect [Gralla et al, 2010]; tendecies and vorteces [Owen et al, 2011].

An empirical Formula for the merger kick

Empirical formula [Campanelli et al '07] for the radiation recoil of generic binary black-hole mergers originally motivated by PN formula [Kidder 1995]

$$\vec{V}_{\rm recoil}(q,\vec{a}_i) = v_m\,\hat{e}_1 + v_\perp(\cos(\xi)\,\hat{e}_1 + \sin(\xi)\,\hat{e}_2) + v_\parallel\,\hat{e}_z,$$

$$q = m_1/m_2, \quad \eta = q/(1+q)^2, \quad \vec{a}_i = \vec{S}_i/m_i^2$$

$$v_m = A\eta^2\sqrt{1-4\eta}(1+B\eta)$$

in-plane kick < 175 km/s [Fitchett '83, Gonzalez et al 07]

$$v_\perp = H\frac{\eta^2}{(1+q)}\left(a_2^\parallel - q a_1^\parallel\right)$$

in-plane kick < 500 km/s [Baker et al 07, Hermann et al '07, Koppitz et al '07]. See [Pollney et al 2007] for quadratic corrections in the spins. Also, work in progress by RIT …

$$v_\parallel = K\frac{\eta^2}{(1+q)}\cos(\Theta-\Theta_0)\left|\vec{a}_2^\perp - q\vec{a}_1^\perp\right|$$

out-of-plane kick < 4,000 km/s [Campanelli et al 07, Lousto et al '08]. See also [Baker et al '08] for a modification of mass scaling ($\eta^2 \rightarrow 4\eta^3$) …

- ξ angle between unequal-mass and spin contributions to recoil in the orbital plane
- Θ angle between in-plane $\vec{\Delta} \equiv (m_1+m_2)(\vec{S}_2/m_2 - \vec{S}_1/m_1)$ and infall direction at merger

Remnant BH masses and spins

What is the cosmological distribution of masses and spins? (related to distribution of recoils)
What is the final mass and spins from generic mergers?
Is cosmic-censorship obeyed?

- Models of remnant BH masses and spins:
  - Early efforts via Lazarus [Baker et al. 2004]
  - Empirical fitting models [Campanelli et al. 2006; Rezzolla et al. 2009; Tichy & Marronetti 2008, Healy et al, 2009]
  - Physically motivated models with fitting functions [Boyle & Kesden 2008, Buonanno et al. 2008, Kesden 2008, ..
  - Empirical formulas based on PN-inspired parametrization [Lousto, Campanelli & Zlochower, arXiv: 0904.3541]:

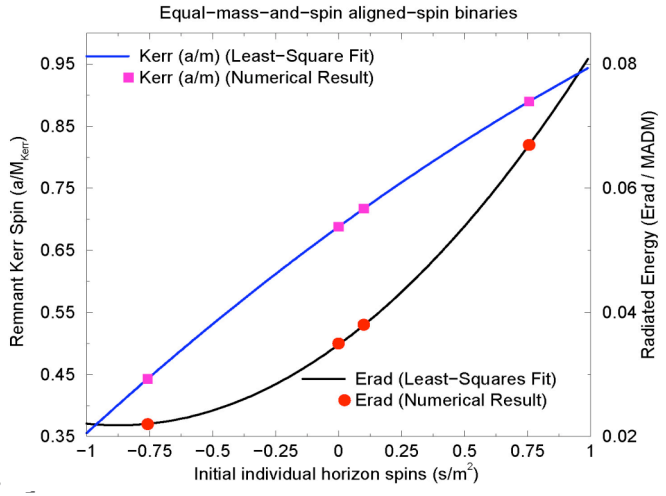

[Campanelli et al, PRD73, 2006]

$$\delta M/M = \eta\,\tilde{E}_{ISCO} + E_2\eta^2 + E_3\eta^3 + \frac{\eta^2}{(1+q)^2}\Big\{E_S\,(\alpha_2^{\parallel} + q^2\,\alpha_1^{\parallel}) + E_\Delta\,(1-q)\,(\alpha_2^{\parallel} - q\,\alpha_1^{\parallel}) + E_A\,|\vec{\alpha}_2 + q\vec{\alpha}_1|^2 + E_B\,|\alpha_2^{\perp} + q\alpha_1^{\perp}|^2\,(\cos^2(\Theta_+ - \Theta_2) + E_C) + E_D\,|\vec{\alpha}_2 - q\vec{\alpha}_1|^2 + E_E\,|\alpha_2^{\perp} - q\alpha_1^{\perp}|^2\,(\cos^2(\Theta_- - \Theta_3) + E_F)\Big\}, \qquad (2)$$

$$\vec{\alpha}_{\rm final} = (1-\delta M/M)^{-2}\Big\{\eta\tilde{\vec{J}}_{ISCO} + (J_2\eta^2 + J_3\eta^3)\,\hat{n}_{\parallel} + \frac{\eta^2}{(1+q)^2}\Big(\Big[J_A\,(\alpha_2^{\parallel} + q^2\,\alpha_1^{\parallel}) + J_B\,(1-q)\,(\alpha_2^{\parallel} - q\,\alpha_1^{\parallel})\Big]\,\hat{n}_{\parallel} + (1-q)\,|\vec{\alpha}_2^{\perp} - q\,\vec{\alpha}_1^{\perp}|\sqrt{J_\Delta\cos[2(\Theta_\Delta - \Theta_4)] + J_{M\Delta}}\,\hat{n}_{\perp} + |\vec{\alpha}_2^{\perp} + q^2\,\vec{\alpha}_1^{\perp}|\,\sqrt{J_S\cos[2(\Theta_S - \Theta_5)] + J_{MS}}\,\hat{n}_{\perp}\Big)\Big\}. \qquad (4)$$

- **Merging equal-mass BH binaries, with maximal spins aligned with orbital angular momentum produce a remnant BH with final spin a/M ~ 0.96 - 0.98**
  no naked singularities so far!

Motivations to study IMRBHBs

- Apart from the purely theoretical aspects, comparison with GSF
- Supermassive BH collisions come with mass ratios 1/10 – 1/100 in cosmological scenarios
- Galactic BHB involving *intermediate mass* BHs (~1000Msun) involve IMR encounters
- As a first comparison to a galactic BH/NS merger.
- To seek an approximate template bank waveform generator for AdvLigo and 3G detectors.

Can we simulate Small Mass Ratio Black-Hole Binaries?
Yes, we can!

- Low mass ratio binaries first explored in [Baker et al. 2008 (q = 1/6), Gonzalez et al, 2009 (q = 1/10), Lousto & Zlochower, 2009 (q = 1/8 spinning)].

- Simulations of IMR black-hole Binaries for q=1/10, 1/15,1/100 [Lousto et al, 2010]

- Adapt the gauge of the moving punctures approach with a variable damping term for the shift, based on the small q gauge proposed in [Mueller & Bruegmann, 2010]

$$(\partial_t - \beta^i \partial_i)\alpha = -2\alpha K,$$
$$\partial_t \beta^a = \frac{3}{4}\tilde{\Gamma}^a - \eta(x^k,t)\,\beta^a,$$

$$\eta(x^k,t) = R_0 \frac{\sqrt{\partial_i W \partial_j W \tilde{\gamma}^{ij}}}{(1-W^a)^b},$$

- Derived an extrapolation (to infinite radius) formula for the waveform extracted at finite radius.

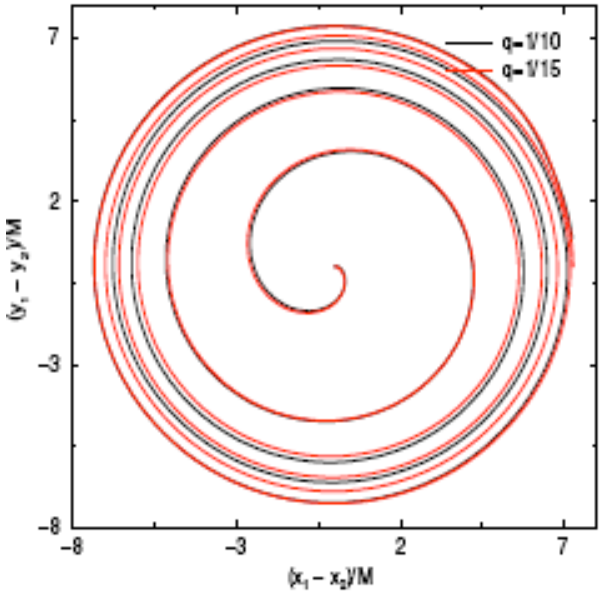

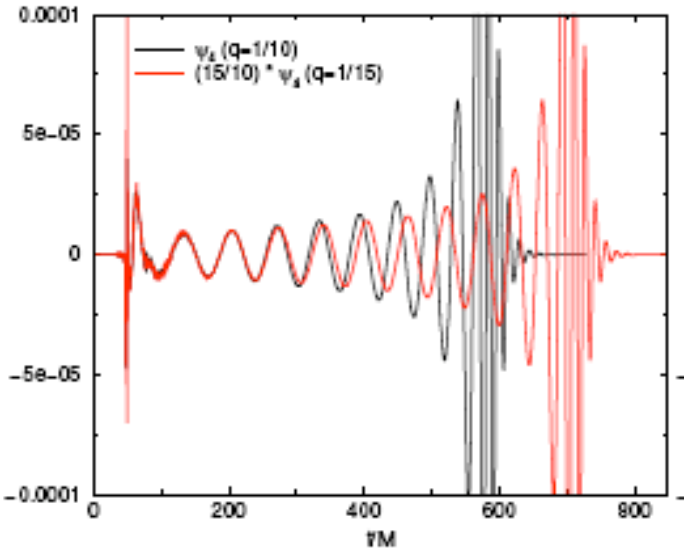

[Lousto, Nakano, Zlochower, Campanelli, PRD. 2010, arXiv:1008.4360]

Simulation of a 1:100 Black-Hole Binary

- Obtain 2 orbits inside ISCO,
  - iterative procedure for quasi-circular orbit initial data (based on Caltech-Cornell method).
- Very challenging numerics due to different 4 different scales: small BH, large BH, inter-BH dynamics, radiation scale.
- Require modified gauge conditions (to resolve dynamics between BHs and far regions)
- Evolutions for 20,000M in terms in terms of the small BH
  - CFL condition requires time-step be set by smallest of these scales (small BH)

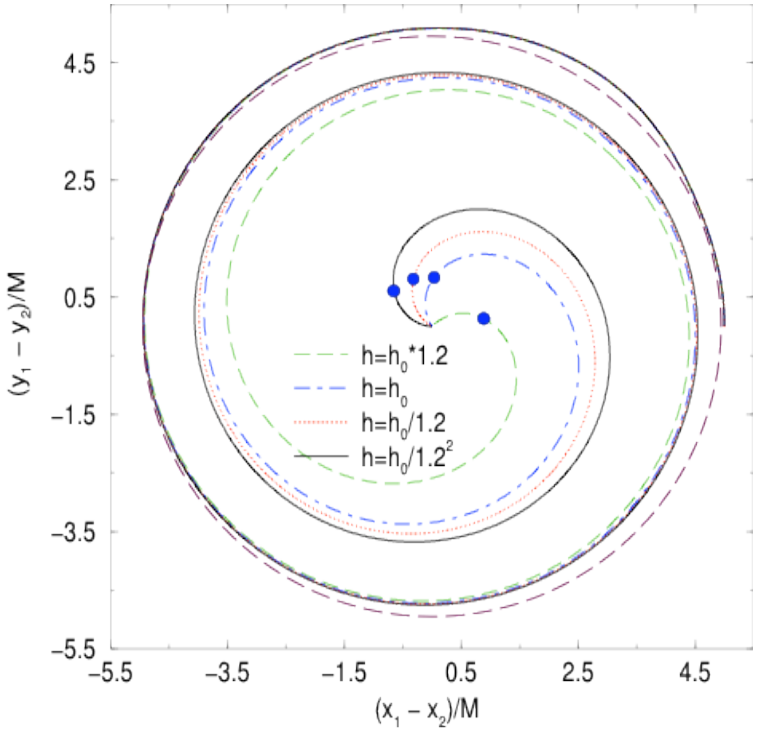

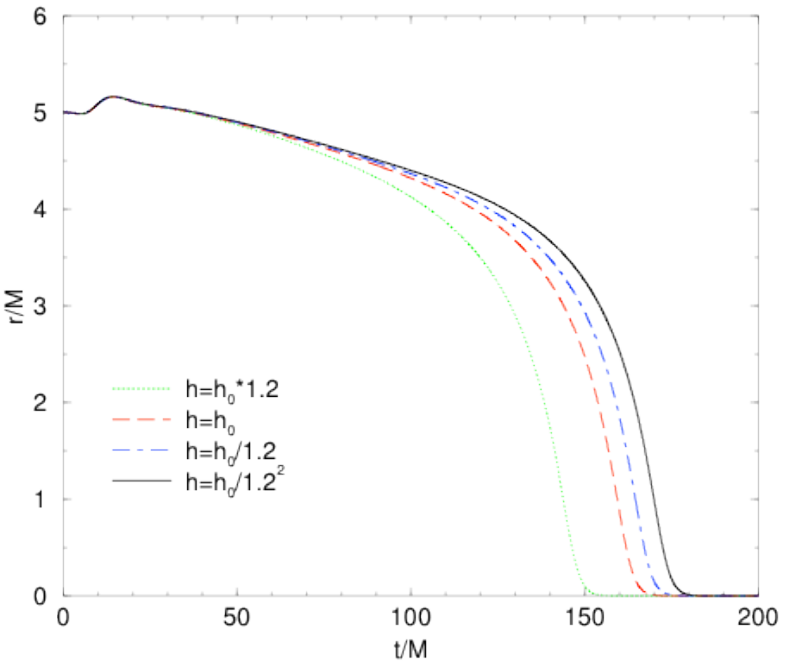

[Lousto and Zlochower, Phys. Rev. Lett. arXiv: 1009.0292]

How we did it.I: Gauge

$$(\partial_t - \beta^i \partial_i)\alpha = -2\alpha K, \quad (1)$$

$$\partial_t \beta^a = \frac{3}{4}\tilde{\Gamma}^a - \eta(x^k, t)\,\beta^a, \quad (2)$$

$$\eta(x^k, t) = R_0 \frac{\sqrt{\tilde{\gamma}^{ij}\partial_i W \partial_j W}}{(1 - W^a)^b}, \quad (3)$$

(a,b)= (2,2) is our preferred gauge. The original (1,2) leads to instabilities. (1,1) and (2,1) enhance grid noise and lowers gauge speed waves.

η(x,y)

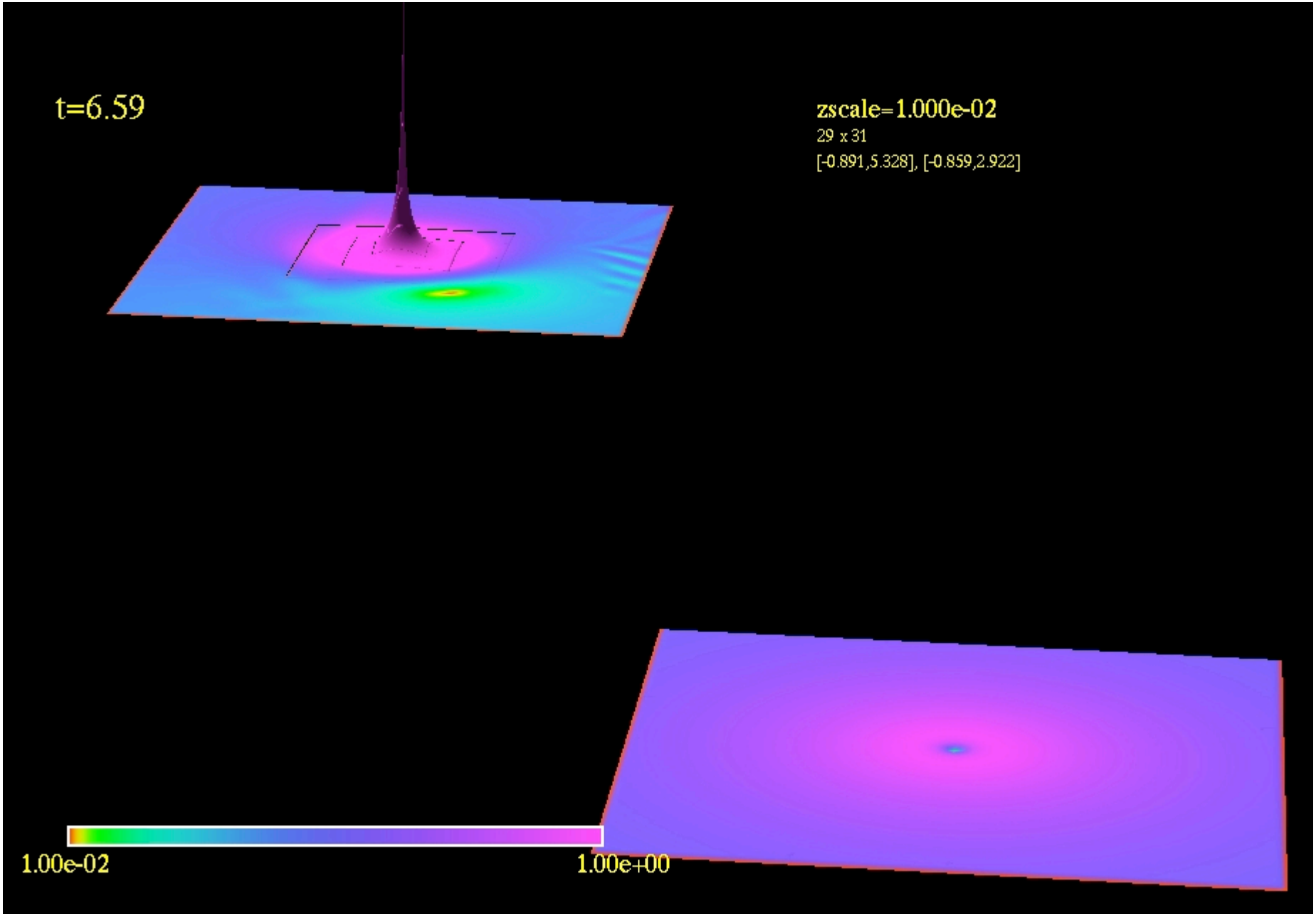
t=6.59
zscale=1.000e-02
29 x 31
[-0.891,5.328], [-0.859,2.922]
1.00e-02
1.00e+00

How we did it.II: AMR Grid structure

(±) parity effective potentials of a Schwarzschild BH can be written as

$$V_\ell^{\pm} = \pm 6M \frac{df}{dr^\star} + (6M)^2 f^2 + 4\lambda(\lambda+1) f, \qquad (4)$$

where

$$f = \frac{(r-2M)}{2r^2(\lambda r + 3M)}, \quad \lambda = \frac{1}{2}(\ell+2)(\ell-1). \qquad (5)$$

$$\frac{d(V_\ell^+ + V_\ell^-)}{dR} = 0, \quad r = R\left(1+\frac{M}{2R}\right)^2, \qquad (6)$$

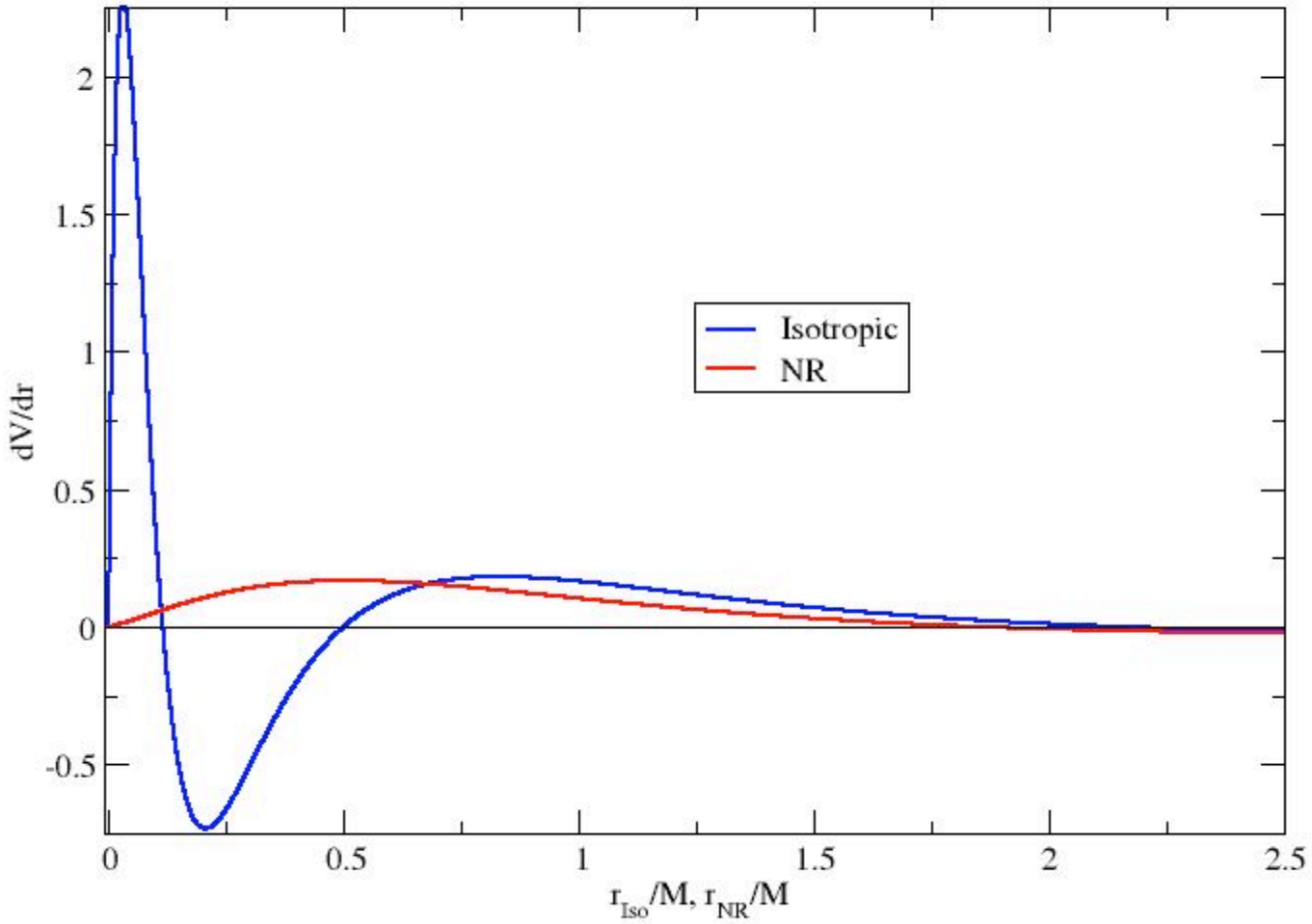

The zeroes of dV/dr are located at $R_H/4$, R_H, and $4R_H$.
We use this to set our refinement levels. grid.avi

How we did it.III: Computational resources

- Requires very large simulations on (up to) 1,024 processors
- Large memory usage 2 TB ram
- Long term runs for (up to) 3 months

Results.I: Trajectories

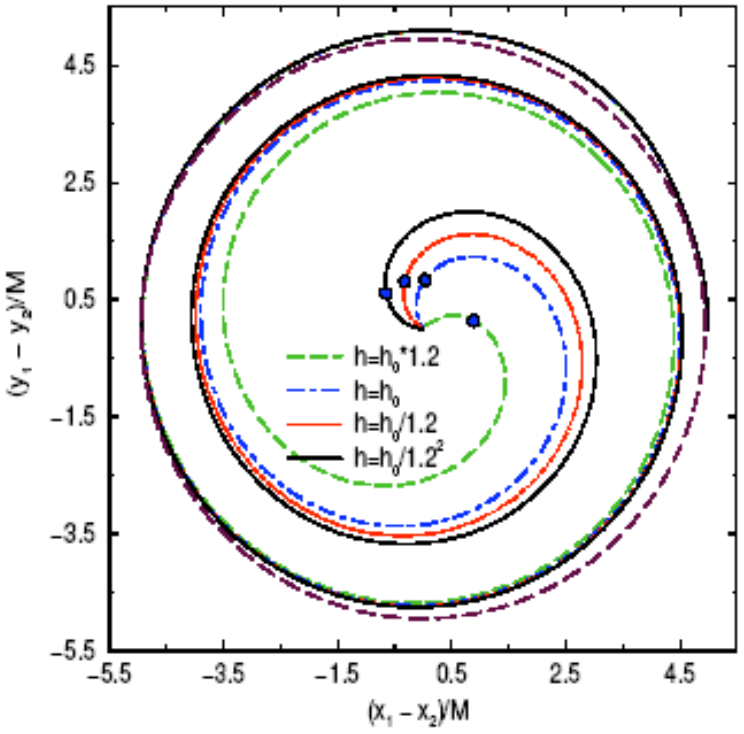

FIG. 1: An xy projection of the trajectories for the two highest resolutions of the $q = 1/100$ configuration. The dotted circle corresponds to the ISCO radius while the small filled in circle corresponds to the point on the trajectory where a common horizon is first detected. Note the initial "jump" in radius (see Fig. 2) due to the initial data radiation content.

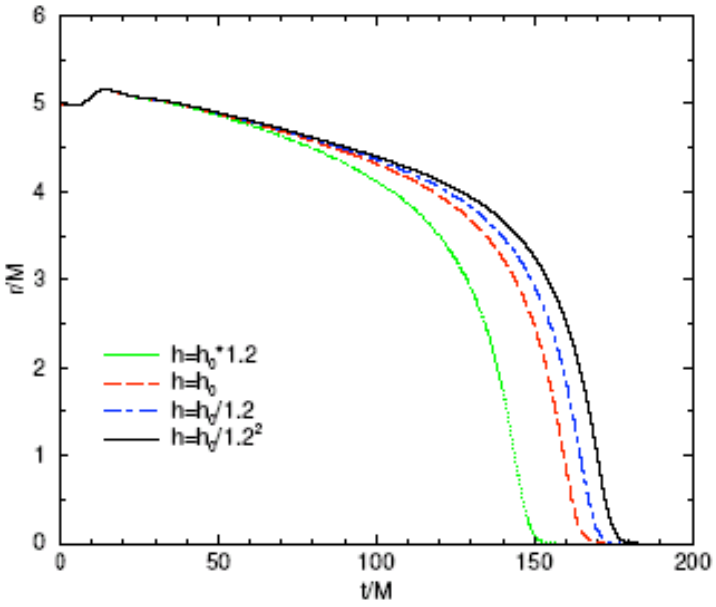

FIG. 2: The orbital radius as a function of time and resolution for the $q = 1/100$ configuration. Note the initial "jump" in the orbit due to the initial data.

h2o_with_timeLine_and_zoom

Results.IIa: Waveforms

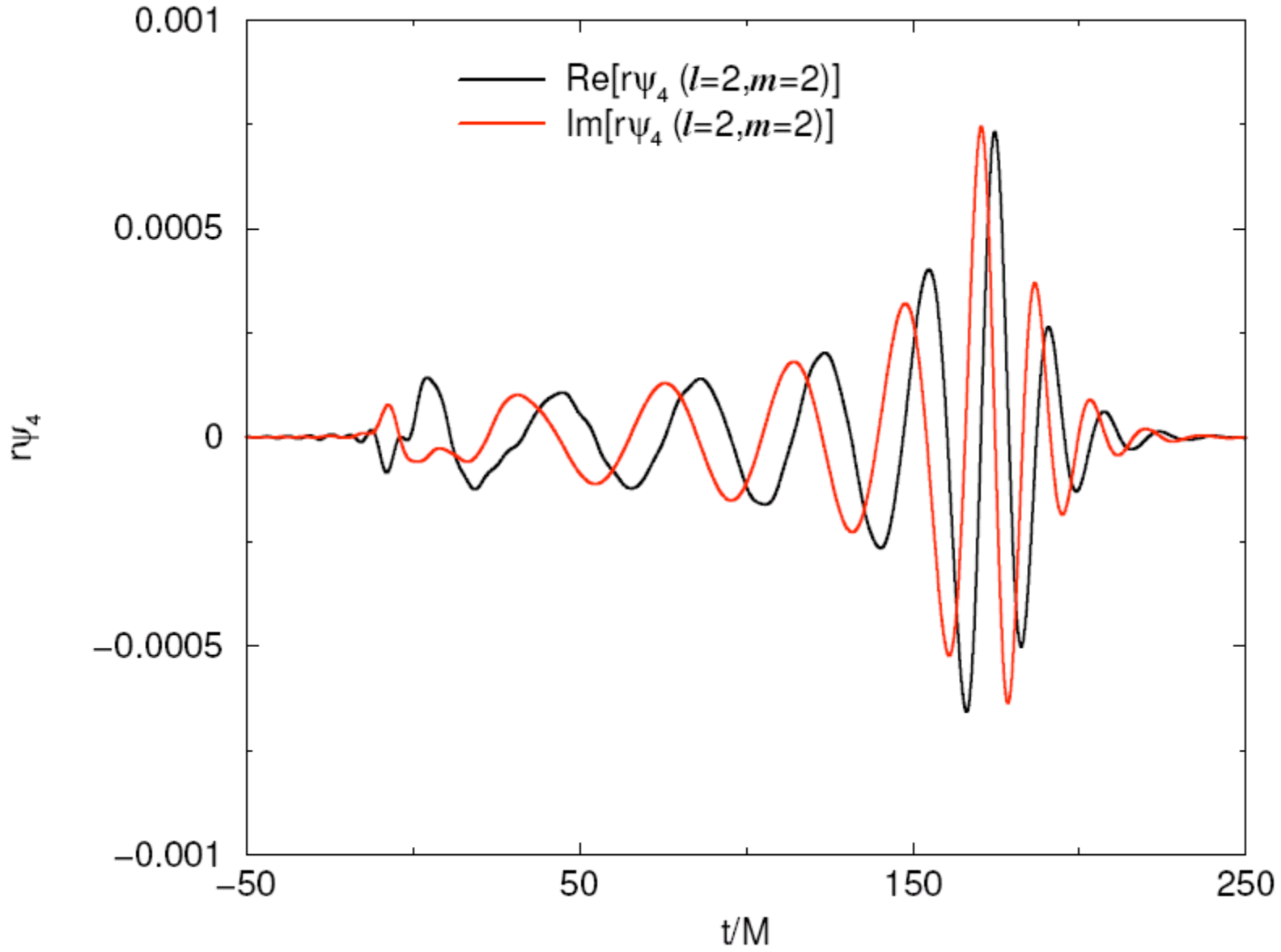

Results.IIb: Waveforms

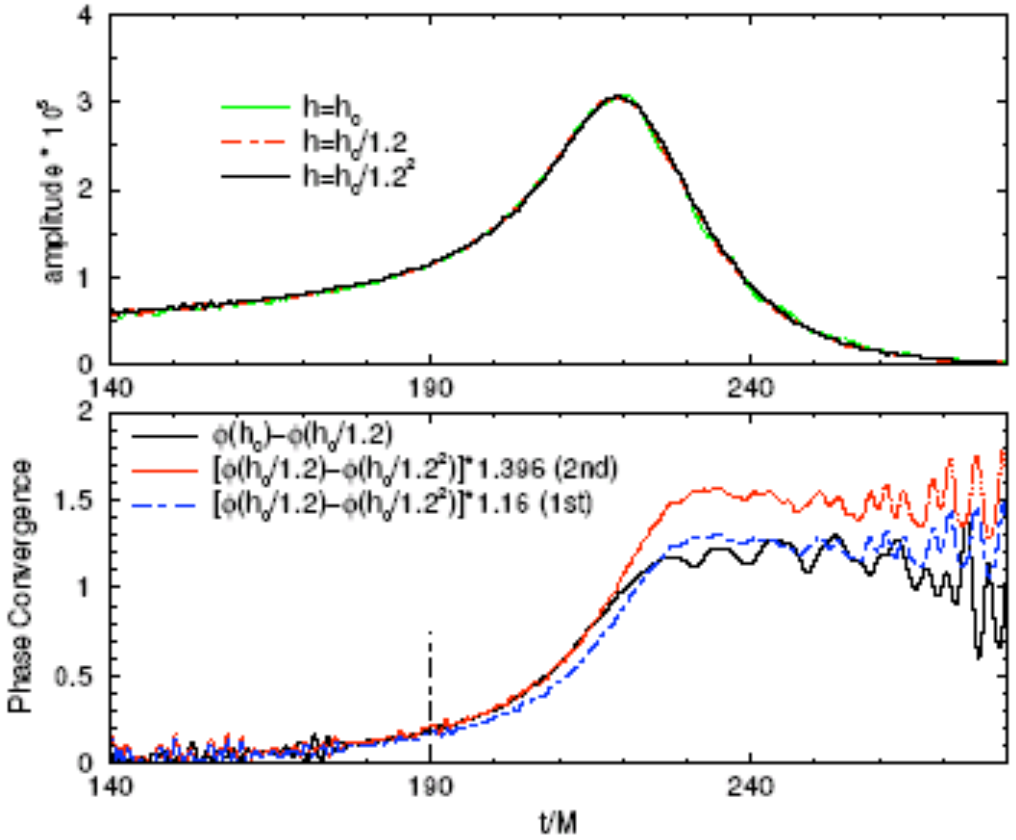

ε_A<0.1%

ε_ϕ<0.1rad

FIG. 3: Convergence of the amplitude and phase of the ($\ell = 2, m = 2$) mode of ψ_4. The phase converges to 2nd order prior to the peak in the amplitude. The vertical line shows the point when $\omega = 0.2$. Note the good agreement in amplitude (the curves have been translated).

Results.III: Comparison with perturbations

The amount of energy and angular momentum radiated when the $(2,2)$ mode frequency is larger than $M\omega_{2,2} > 0.167$ is given by (adding up to $\ell = 4$ modes) $\delta E/M = 0.000047 \pm 0.000001$ and $\delta J/M^2 = 0.00034 \pm 0.00001$, which agrees to within 4% with the particle limit predictions of $\delta E/M = 0.47\eta^2$ and $\delta J/M^2 = 3.44\eta^2$

from ω = 0.167 on (Nagar & Bernuzzi, 2010)

Results.IV: Comparison with q~1 predictions

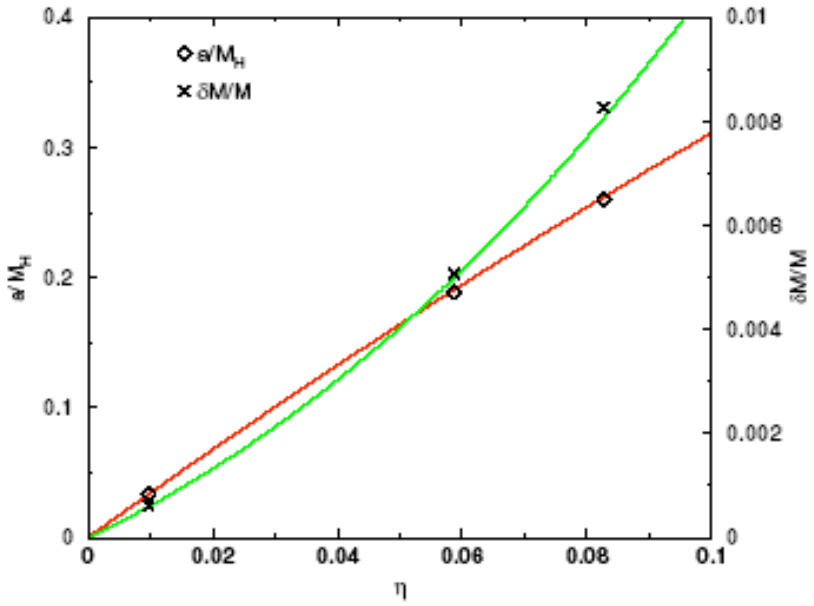

FIG. 4: The remnant spin a/M_H and the radiated mass from infinite separation $\delta M/M$, as a function of the symmetric mass ratio $\eta = q/(1+q)^2$, for $q = 1/10$, $1/15$, $1/100$, as well as the empirical formula prediction.

TABLE III: Remnant spin and total radiated mass (starting from infinite separation) as a function of mass ratio q as measured in our simulations and as predicted by our empirical formulae [32].

q	1/10	1/15	1/100
α (Computed)	0.2603	0.18875	0.0333
α (Predicted)	0.2618	0.1903	0.03358
δM (Computed)	0.00826	0.00507	0.000618
δM (Predicted)	0.00806	0.00498	0.000604

Conclusions for 100:1

- Computational resources
  - Ranger: 100 days runs, 1MSU
  - Local cluster: 20 nodes, still 100 days
  - New computers: ½ this times

- q<1/100 is possible!
  - Going from q=1/10 to q=1/100 did not take 1/q^4 or 1/q^5, but 1/q-times as much resources.
  - Looking forward to self-force comparisons (as we now do regularly with PN for comparable masses)

h2o_with_time.mov

h2o_real_size.mov

h2o_fast.mov

Intertwining Numerical Relativity and Perturbative Techniques

[Lousto, Nakano, Zlochower, Campanelli, PRD 2010, arXiv:1008.4360]

•Feed NR trajectories for small mass ratio (e.g. q=1/10,1/15,1/100), transformed in the Schwarzschild gauge, in the source terms of the Regge-Wheller-Zerilli Schwarzschild perturbations formalism

•Use more efficient perturbative evolutions to compute waveforms at large radii, as a function of the trajectory (and *q)*

$$\left[-\frac{\partial^2}{\partial t^2}+\frac{\partial^2}{\partial r^{*2}}-V_\ell^{(\mathrm{even})/(\mathrm{odd})}(r)\right]\psi_{\ell m}^{(\mathrm{even})/(\mathrm{odd})}(t,r)$$
$$=S_{\ell m}^{(\mathrm{even})/(\mathrm{odd})}[r_p(t),\Phi_p(t)]\,, \qquad (1$$

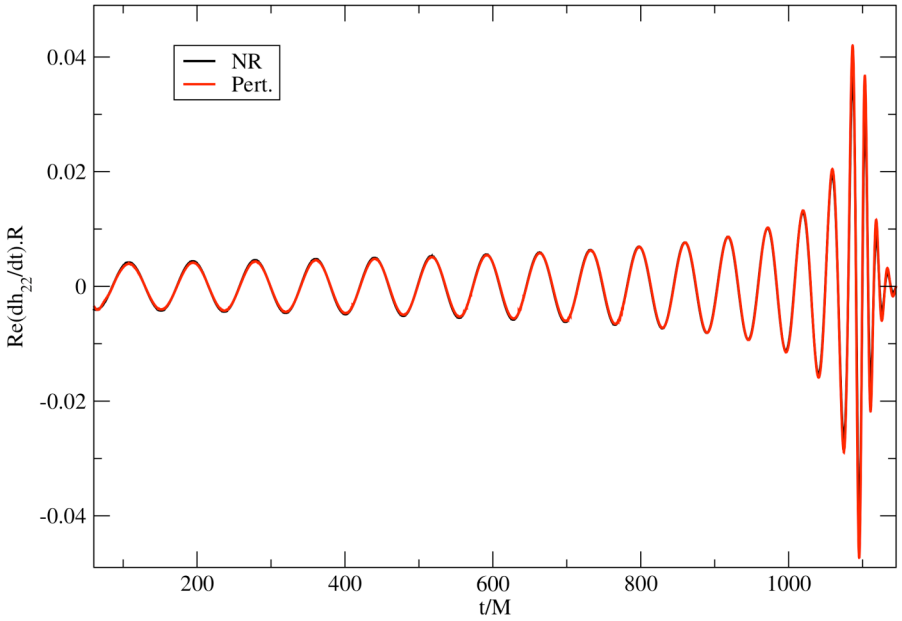

• Remnant spin introduced perturbatively (spin ON)

• Interpolate results to smaller *q*

TABLE I: The overlap between the NR and perturbative dh/dt for the $q = 1/100$ case. The integration time is from $t/M = 75$ to 180 and the definition of the matching is given in Eqs. (26) and (27) of [4]. **Note that we fixed the time translation by only one point for the $(\ell = 2, m = 2)$ mode of dh/dt. Although the phase matching for the Spin ON is better than that of the Spin OFF, the amplitude difference also affect the overlap calculation.**

Mode	$\Re(\ell=2,m=2)$	$\Re(\ell=2,m=1)$	$\Re(\ell=3,m=3)$
Overlap (Spin OFF)	0.998182369	0.998147213	0.997762863
Overlap (Spin ON)	0.998075618	0.998285091	0.998434882
Mode	$\Im(\ell=2,m=2)$	$\Im(\ell=2,m=1)$	$\Im(\ell=3,m=3)$
Overlap (Spin OFF)	0.998201327	0.998098632	0.997741015
Overlap (Spin ON)	0.998085632	0.998225440	0.998432740

Regge-Wheeler-Zerilli formalism with spin (SRWZ)

We then extend this perturbative formalism to take into account small intrinsic spins of the large black hole, and validate it by computing the quasinormal mode (QNM) frequencies, where we find good agreement for spins |a/M|<0.3.

$$G^{(1)}_{\mu\nu}[h^{(1)}] + G^{(1)}_{\mu\nu}[h^{(2)}] + G^{(2)}_{\mu\nu}[h^{(1)}, h^{(1)}]$$
$$= 8\,\pi\,\left(T^{(1)}_{\mu\nu} + T^{(2)}_{\mu\nu}\right) = 8\,\pi\,T_{\mu\nu}\,,$$

$$G^{(1)}_{\mu\nu}[h^{(1,\mathrm{wave})}] \;=\; 8\,\pi\,T_{\mu\nu}\,,$$
$$G^{(1)}_{\mu\nu}[h^{(2,\mathrm{wave})}] \;=\; -G^{(2)}_{\mu\nu}[h^{(1,\mathrm{wave})}, h^{(1,\mathrm{spin})}]\,,$$

mode couplings between the first order and spin

$$-\frac{\partial^2}{\partial t^2}\Psi_{\ell m}(t,r) + \frac{\partial^2}{\partial r^{*2}}\Psi_{\ell m}(t,r) - V^{(\mathrm{even})}_{\ell}(r)\Psi_{\ell m}(t,r)$$
$$+i\,S\,m\,P^{(\mathrm{even},1)}_{\ell}(r)\frac{\partial}{\partial t}\Psi_{\ell m}(t,r) + i\,S\,m\,P^{(\mathrm{even},2)}_{\ell}(r)\frac{\partial^2}{\partial t\partial}$$
$$= S\sqrt{\frac{(\ell-m)\,(\ell+m)}{(2\,\ell-1)\,(2\,\ell+1)}}\,Q^{(\mathrm{even},-)}_{\ell}(r)\Psi^{(\mathrm{o},1)}_{\ell-1\,m}(t,r)$$
$$+S\sqrt{\frac{(\ell+m+1)\,(\ell-m+1)}{(2\,\ell+1)\,(2\,\ell+3)}}\,Q^{(\mathrm{even},+)}_{\ell}(r)\Psi^{(\mathrm{o},1)}_{\ell+1\,m}(t,r) + S^{(\mathrm{even,L})}_{\ell m}(t,r)\,,$$

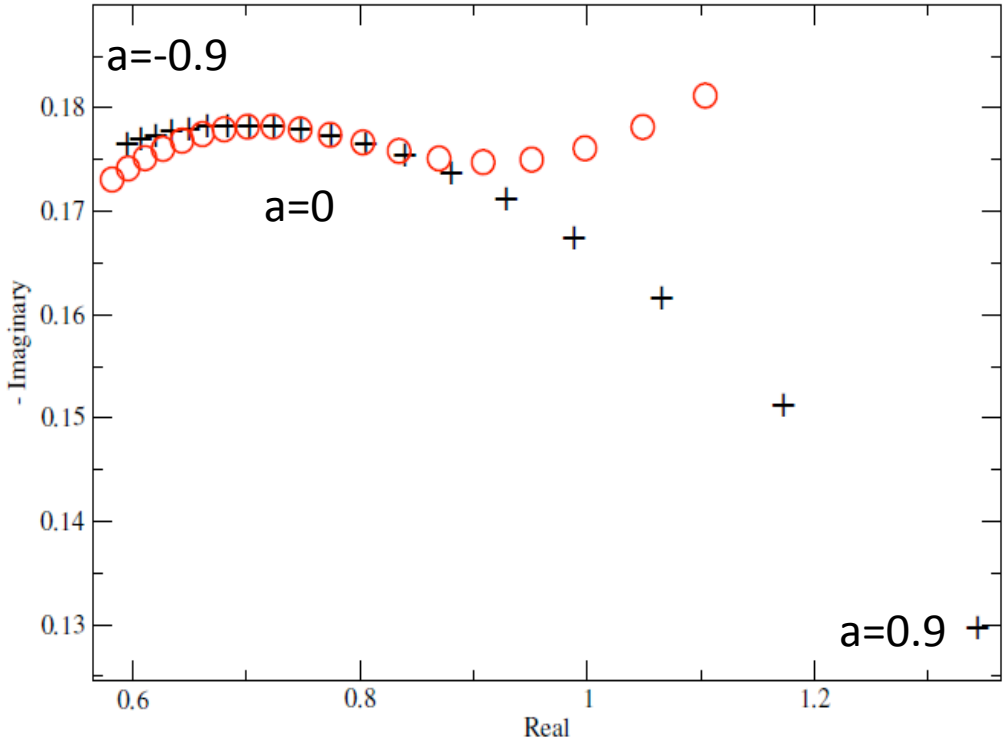

Quasinomal modes

Red: SRWZ
Black: Teukolsky

[Lousto, Nakano, Zlochower, MC, PRD. 2010, arXiv:1008.4360]

Spin perturbations

- q=1/10, (l,m)=(2,2),(2,1),(3,3) with just one track
- Spin a/M=0.26 well captured by perturbations

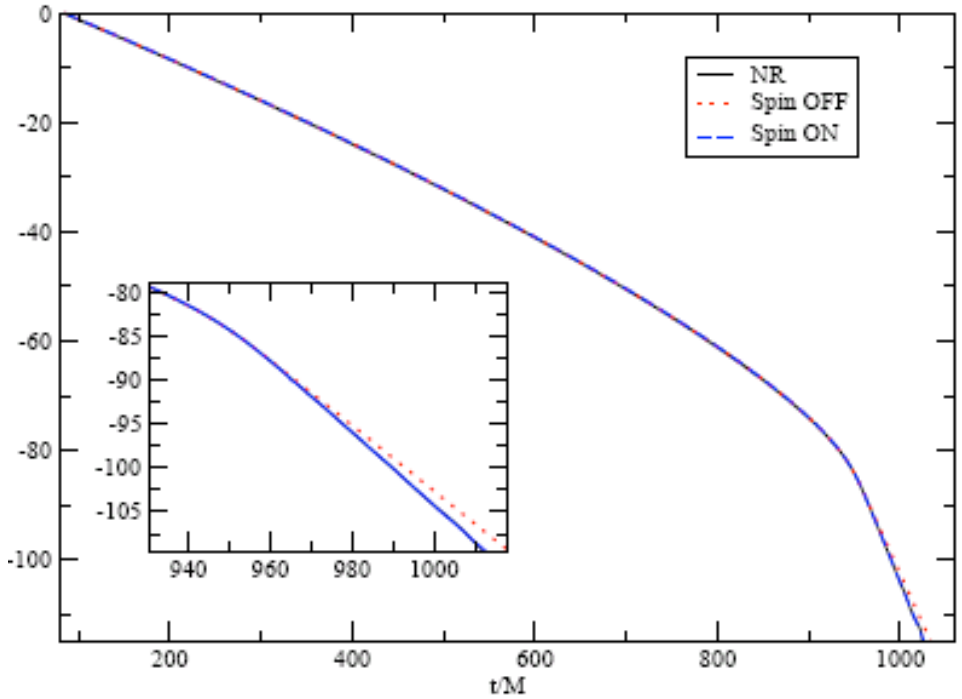

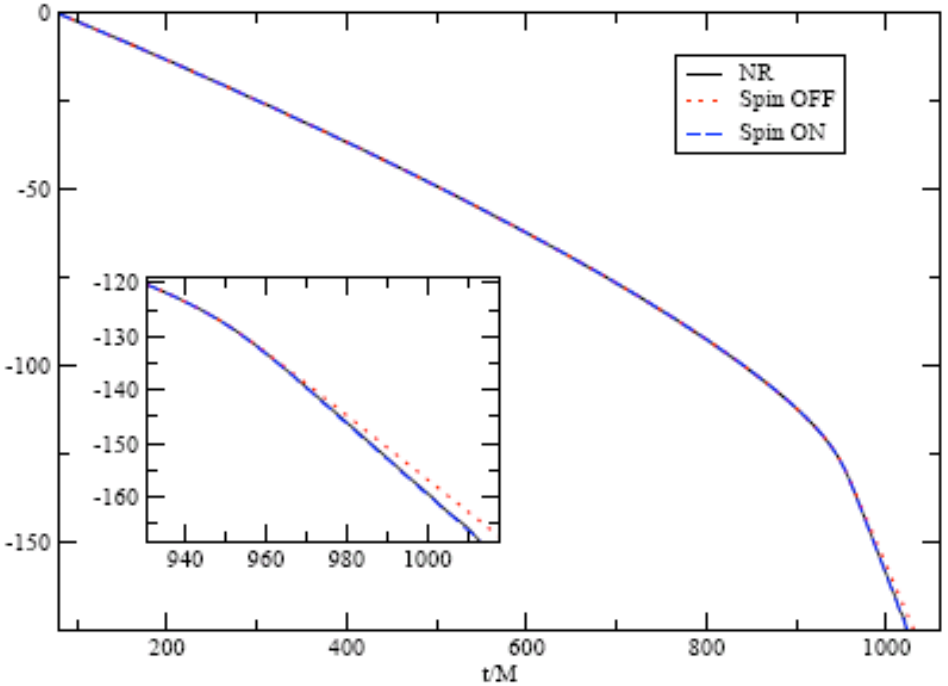

Amplitude errors

- Amplitude Error decreases with q as eta^4/3 at the peak and q^2 at the wings

FIG. 21: *Left*: The amplitude difference for the $q = 1/10$ and $1/100$ case. *Right*: The amplitude difference for the $q = 1/15$ and $1/100$ case.

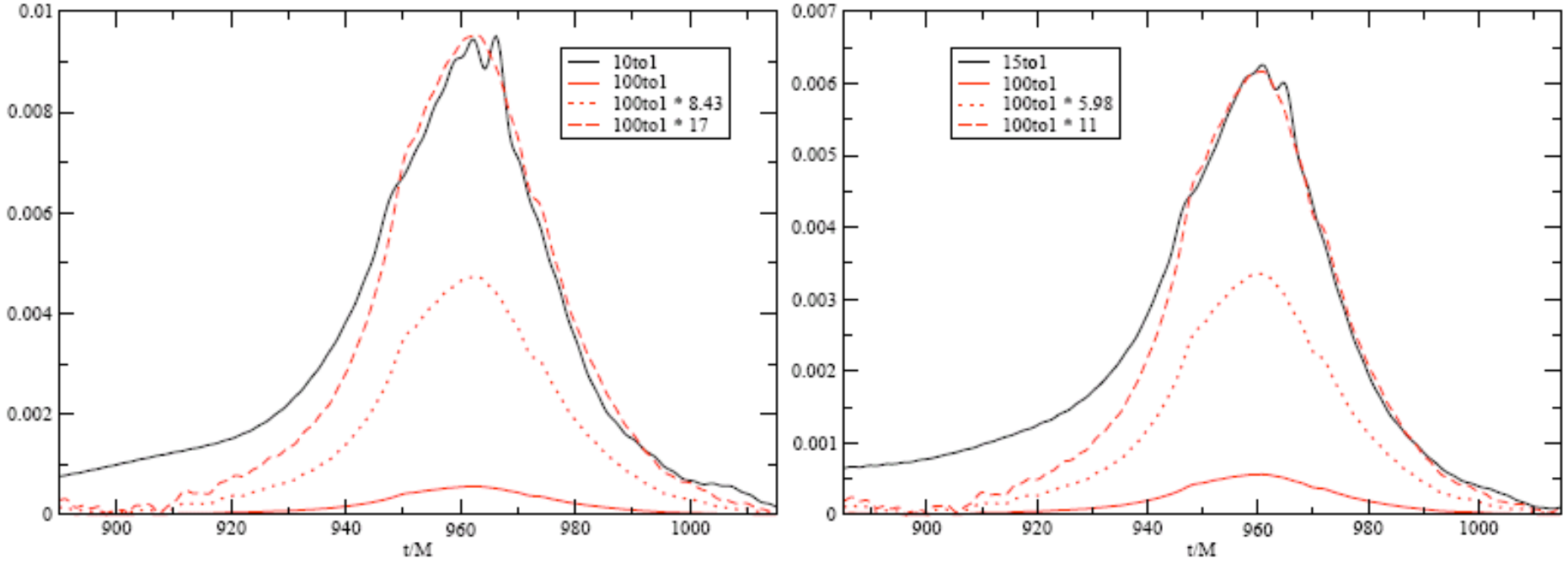

Track Modeling

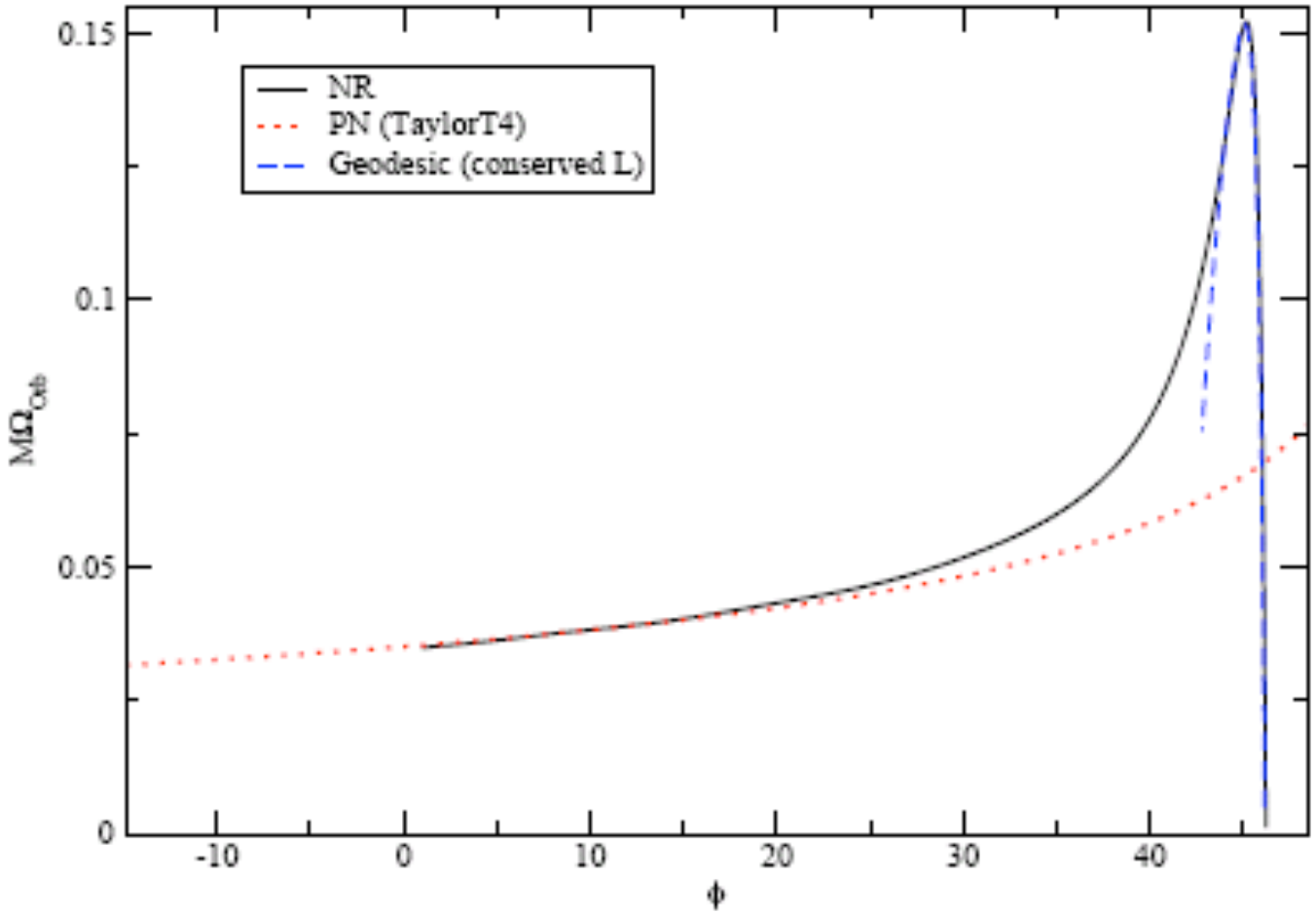

- Track can be described in tandem by PN+NR+Geodesics
- Resembles Lazarus, but in 1D.
- Approach can eventually merge with EOBNR
- Alternative to waveform modeling (Santamaria et al, AEI).

Matching radii for q=1/10

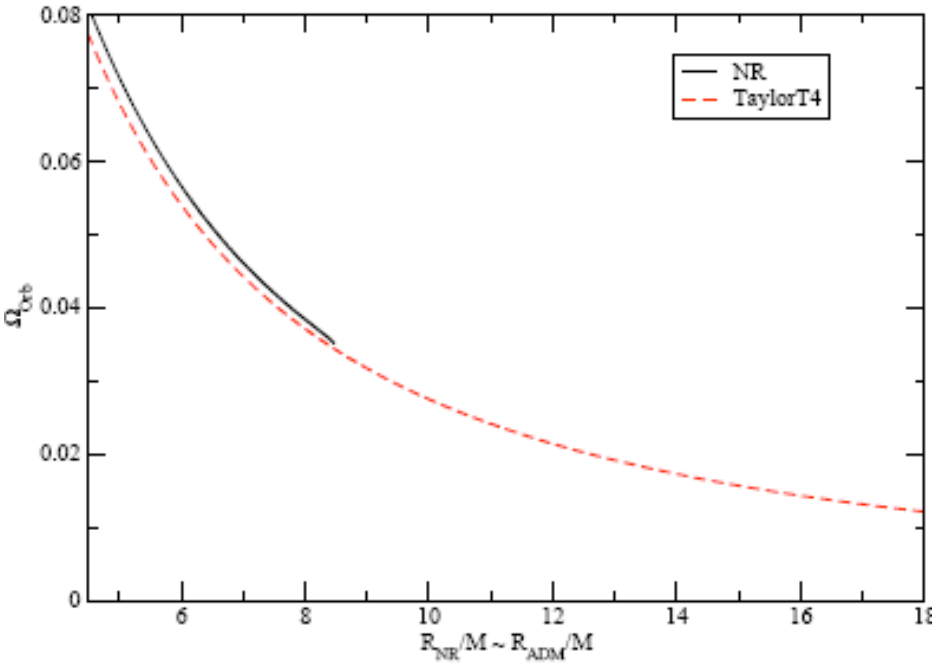

T4 PN matching should work for R>9M

Geodesic matching should work For R<4M

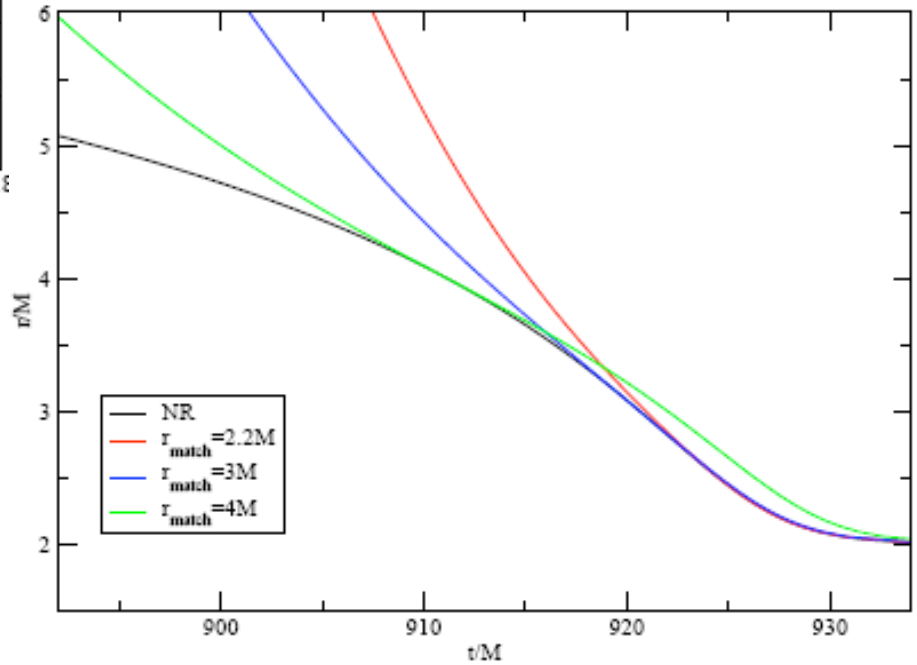

Fitting NR tracks: Phase evolution

For the fitting of the NR evolution, we use the following modified TaylorT4 evolution.

$$
\begin{aligned}
\frac{d\Omega}{dt} = \frac{96}{5}\Omega^{11/3}M^{5/3}\eta\left(1+B\left(\Omega/\Omega_0\right)^{\beta/3}\right)^{-1}\Bigg(1+\left(-\frac{743}{336}-\frac{11}{4}\eta\right)(M\Omega)^{2/3}+4\pi M\Omega \\
+\left(\frac{34103}{18144}+\frac{13661}{2016}\eta+\frac{59}{18}\eta^2\right)(M\Omega)^{4/3}+\left(-\frac{4159}{672}\pi-\frac{189}{8}\eta\pi\right)(M\Omega)^{5/3} \\
+\Bigg(\frac{16447322263}{139708800}+\frac{16}{3}\pi^2-\frac{1712}{105}\gamma-\frac{1712}{315}\ln\left(64\,M\Omega\right)-\frac{56198689}{217728}\eta \\
+\frac{451}{48}\eta\pi^2+\frac{541}{896}\eta^2-\frac{5605}{2592}\eta^3\Bigg)(M\Omega)^2 \\
+\left(-\frac{4415}{4032}\pi+\frac{358675}{6048}\eta\pi+\frac{91495}{1512}\eta^2\pi\right)(M\Omega)^{7/3}+A\left(\Omega/\Omega_0\right)^{\alpha/3}\Bigg),
\end{aligned}
$$

Fitting NR tracks: phase fit 10:1-100:1

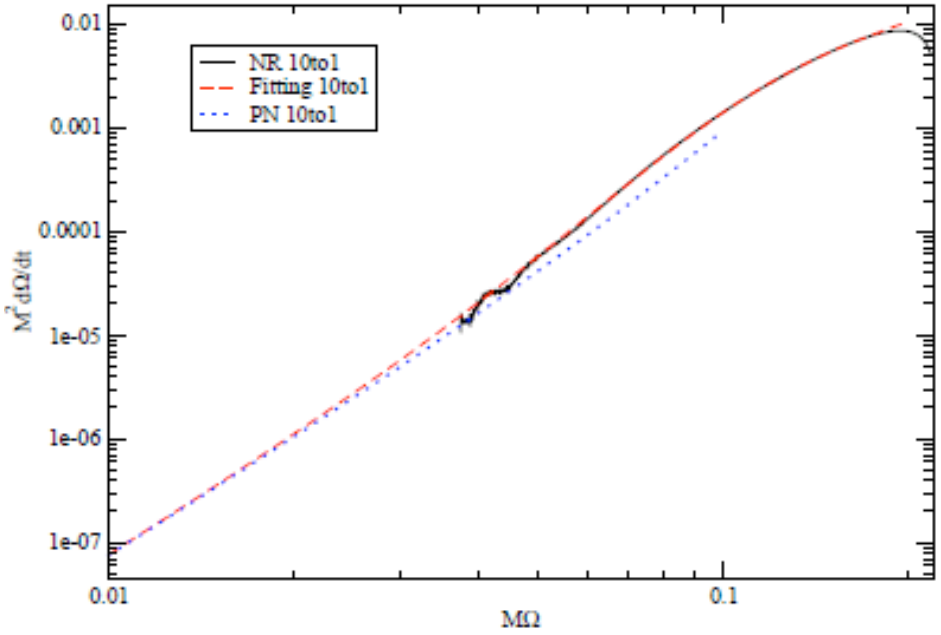

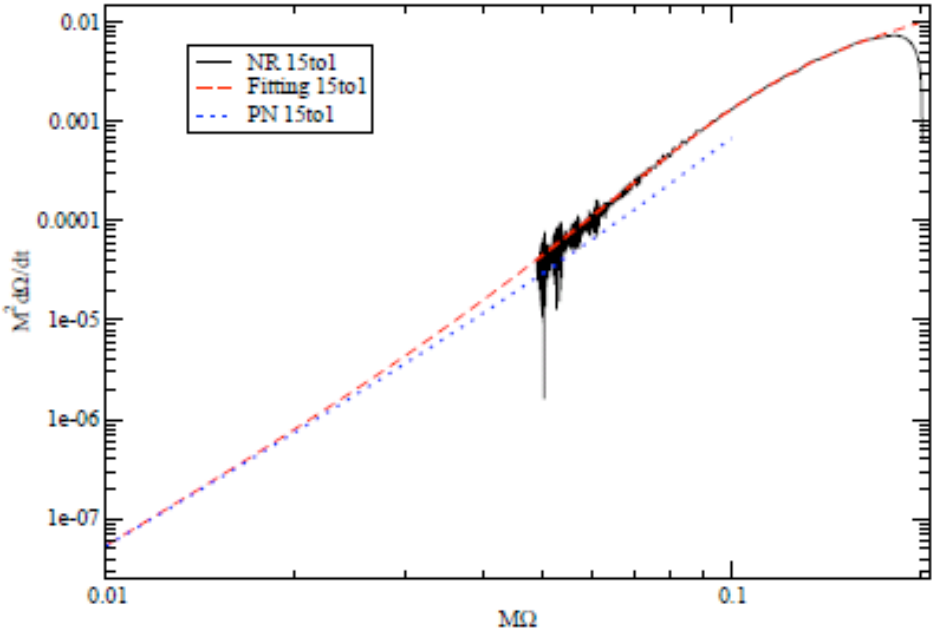

$$
\begin{aligned}
A &= 0.797021\,\eta^{-1.22855}\,, \\
\alpha &= 5.26843\,\eta^{-0.126379}\,, \\
B &= 5.48252\,\eta^{-0.160938}\,, \\
\beta &= 6.80971\,\eta^{-0.244245}\,.
\end{aligned}
$$

Fitting NR tracks: Radial evolution

$$R = \frac{M}{(M\Omega)^{2/3}}\left(1+\left(-1+\frac{1}{3}\,\eta\right)(M\Omega)^{2/3}+\left(-\frac{1}{4}+\frac{9}{8}\,\eta+\frac{1}{9}\,\eta^2\right)(M\Omega)^{4/3}\right.$$
$$\left.+\left(\frac{167}{192}\,\eta\,\pi^2+\frac{2}{81}\,\eta^3-\frac{1}{4}-\frac{1625}{144}\,\eta-\frac{3}{2}\,\eta^2\right)(M\Omega)^2\right)/\left(1+a_0(\Omega/\Omega_0)^{a_1}\right)+C\,,$$

FIG. 43: *Left*: The orbital frequency Ω vs. radius R in the NR coordinates. The right ends of the thick and thin curves show $R_{\rm Sch}=3M$ and $2M$, respectively. **Same as the previous one.** *Right*: The fitting for the 10 : 1 case. **New!**

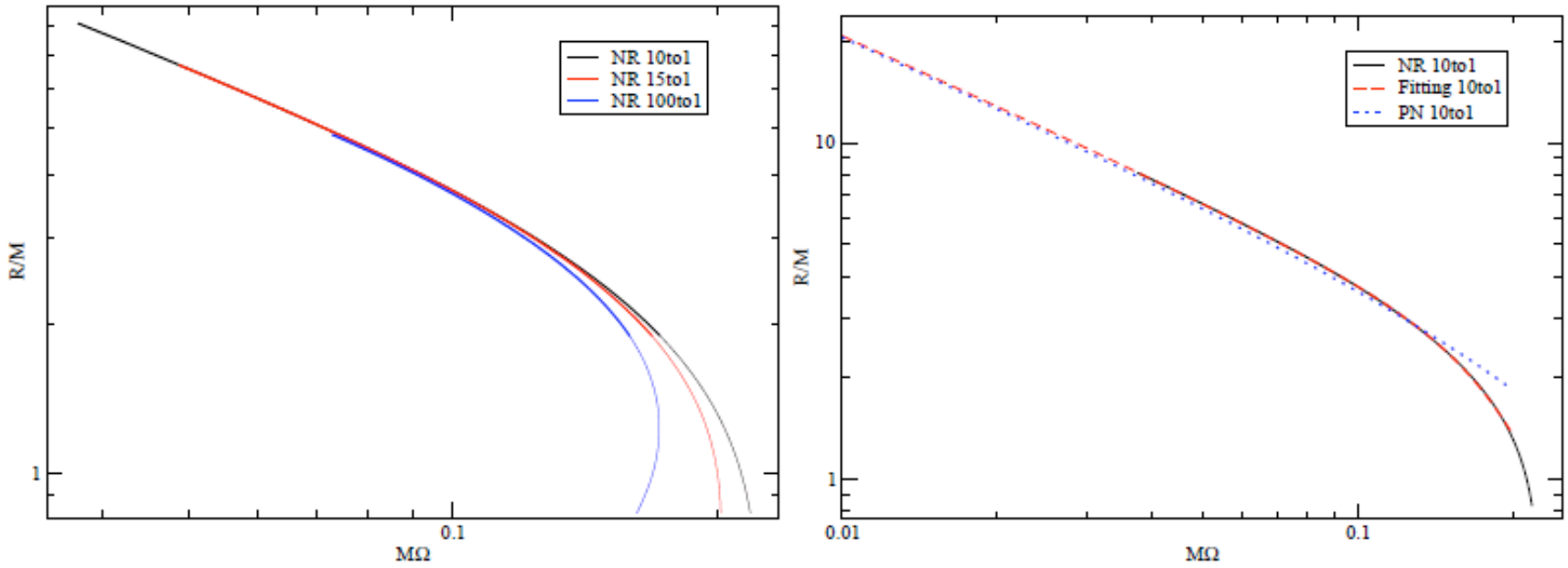

Fitting NR tracks

FIG. 44: *Left*: The fitting for the 15 : 1 case. **New!** *Right*: The fitting for the 100 : 1 case. **New!**

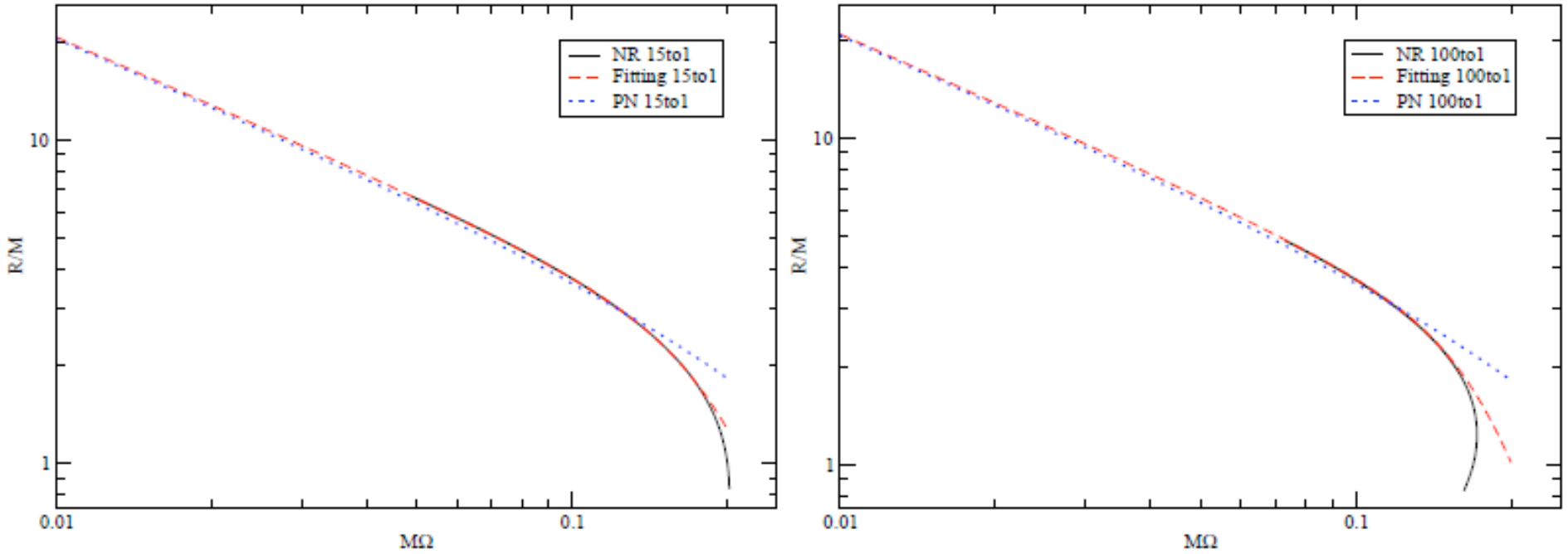

	C	a_0	a_1
10 : 1	0.223202	0.00472378	4.35639
15 : 1	0.238111	0.00507921	4.45613
100 : 1	0.199280	0.00375942	5.17835

Time dependence

$$
\begin{aligned}
t &= \int_{0.034/M}^{\Omega} d\Omega \, \frac{1}{\dot{\Omega}} \\
&= \frac{M^2}{A(q)} \int_{0.034/M}^{\Omega} d\Omega \left(\left(\frac{M\Omega}{0.034} \right)^{-\alpha(q)} + B(q) \left(\frac{M\Omega}{0.034} \right)^{-\alpha(q)+\beta(q)} \right) , \\
R &= R(\Omega) \\
&= M \, \frac{1 + a_0 \left(M\Omega \right)^{2/3} + a_1 \left(M\Omega \right)^{\gamma}}{\left(M\Omega \right)^{2/3}} , \\
\phi &= \int_{0.034/M}^{\Omega} d\Omega \, \frac{\Omega}{\dot{\Omega}} \\
&= \frac{0.034\, M}{A(q)} \int_{0.034/M}^{\Omega} d\Omega \left(\left(\frac{M\Omega}{0.034} \right)^{-\alpha(q)+1} + B(q) \left(\frac{M\Omega}{0.034} \right)^{-\alpha(q)+\beta(q)+1} \right) ,
\end{aligned}
$$

Waveform Comparison

FIG. 33: The amplitude (left) and phase (right) of the $(\ell = 2, m = 2)$ dh/dt for the $q = 1/10$ case. The (black) solid and (red) dashed curves are derived from the NR track and fitting function, respectively.

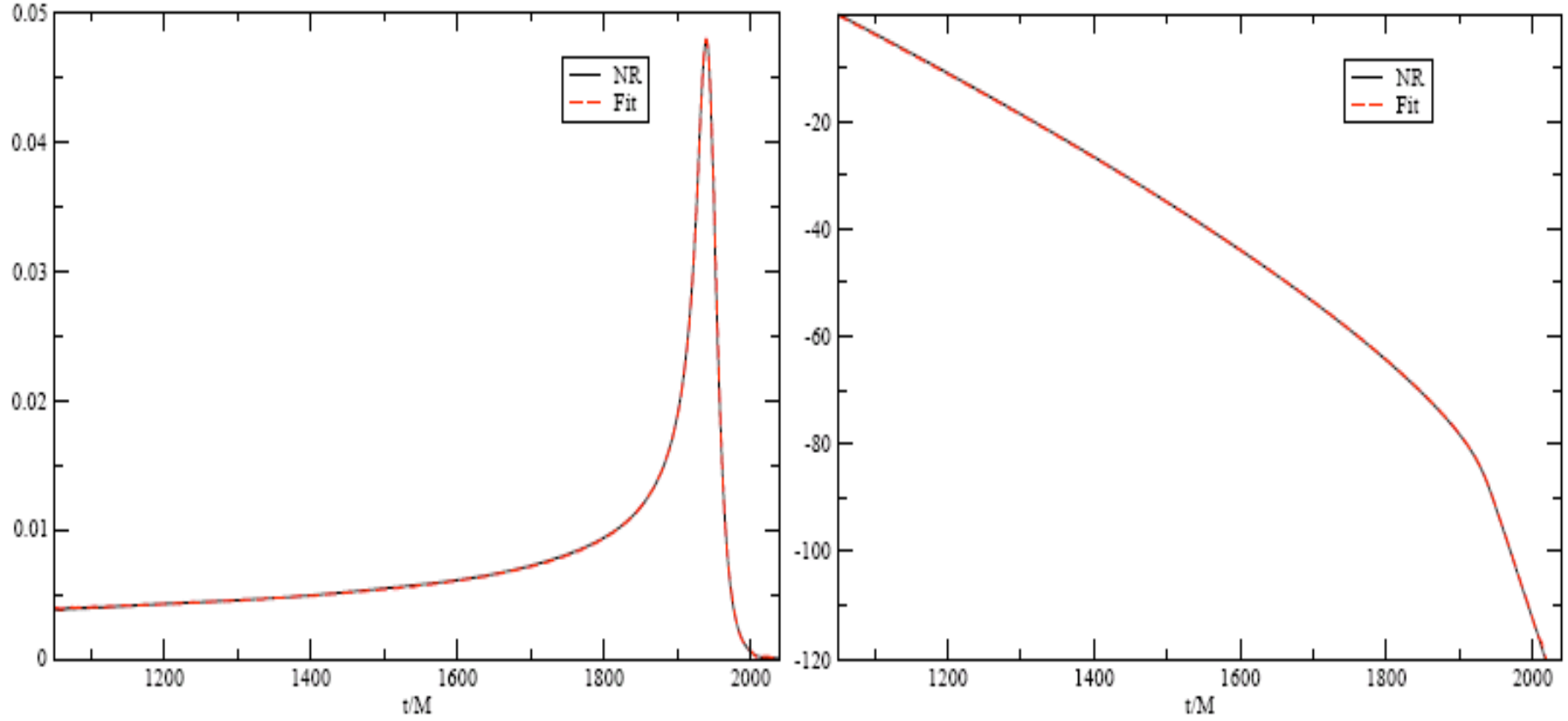

Discussion

- NR Simulations for 0.1<q<0.01 possible, but still though
- Perturbative approach with NR tracks works for waveform generation
  - One track gets all modes (l,m)
  - NR tracks actually needed for separations 10<r/M<4
  - Extraction at arbitrary radii
  - Perturbative code fast and amenable to run in GPUs
- Track modeling with *PN* up to separations 10-12M, then *Full Numerics*, then 'universal' *geodesic.*
- Teukolsky (Hughes et al) and second order perturbations could do the full job. NR simulations with highly spinning hole and q=1/8 done two years ago. Spin effects important for trajectories, not so much for directly modify the radiation locally. [Seen in the spin-on plots above].
- Do we really need higher order corrections to the waveforms?

Fin